1521-0111/95/1/82–96$35.00
MOLECULAR PHARMACOLOGY

https://doi.org/10.1124/mol.118.113514
Mol Pharmacol 95:82–96, January 2019

A Modified Tripeptide Motif of RS1 (*RSC1A1*) Down-Regulates Exocytotic Pathways of Human Na^+-D-glucose Cotransporters SGLT1, SGLT2, and Glucose Sensor SGLT3 in the Presence of Glucose[S]

Nadine Schäfer, Prashanth Reddy Rikkala, Maike Veyhl-Wichmann, Thorsten Keller, Christian Ferdinand Jurowich, Dietmar Geiger,[1] and Hermann Koepsell[1]

Department of Molecular Plant Physiology and Biophysics, Julius-von-Sachs-Institute (N.S., T.K., D.G., H.K.) and Institute of Anatomy and Cell Biology (P.R.R., M.V.-W., H.K.), University of Würzburg, Würzburg, Germany; and Department of General, Visceral, Vascular, and Paedriatic Surgery, University Hospital of Würzburg, Würzburg, Germany (C.F.J.)

Received July 3, 2018; accepted October 19, 2018

ABSTRACT

A domain of protein RS1 (*RSC1A1*) called RS1-Reg down-regulates the plasma membrane abundance of Na^+-D-glucose cotransporter SGLT1 by blocking the exocytotic pathway at the *trans*-Golgi. This effect is blunted by intracellular glucose but prevails when serine in a QSP (Gln-Ser-Pro) motif is replaced by glutamate [RS1-Reg(S20E)]. RS1-Reg binds to ornithine decarboxylase (ODC) and inhibits ODC in a glucose-dependent manner. Because the ODC inhibitor difluoromethylornithine (DFMO) acts like RS1-Reg(S20E), and DFMO and RS1-Reg(S20E) are not cumulative, we raised the hypothesis that RS1-Reg(S20E) down-regulates the exocytotic pathway of SGLT1 at the *trans*-Golgi by inhibiting ODC. We investigated whether QEP down-regulates human SGLT1 (hSGLT1) like hRS1-Reg(S20E) and whether human Na^+-D-glucose cotransporter hSGLT2 and the human glucose sensor hSGLT3 are also addressed. We expressed hSGLT1, hSGLT1 linked to yellow fluorescent protein (hSGLT1-YFP), hSGLT2-YFP and hSGLT3-YFP in oocytes of *Xenopus laevis*, injected hRS1-Reg(S20E), QEP, DFMO, and/or α-methyl-D-glucopyranoside (AMG), and measured AMG uptake, glucose-induced currents, and plasma membrane-associated fluorescence after 1 hour. We also performed in vitro AMG uptake measurements into small intestinal mucosa of mice and human. The data indicate that QEP down-regulates the exocytotic pathway of SGLT1 similar to hRS1-Reg(S20E). Our results suggests that both peptides also down-regulate hSGLT2 and hSGLT3 via the same pathway. Thirty minutes after application of 5 mM QEP in the presence of 5 mM D-glucose, hSGLT1-mediated AMG uptake into small intestinal mucosa was decreased by 40% to 50%. Thus oral application of QEP in a formulation that optimizes uptake into enterocytes but prevents entry into the blood is proposed as novel antidiabetic therapy.

Introduction

Previously we showed that intracellular protein RS1 (*RSC1A1*) is critically involved in the posttranslational regulation of the Na^+-D-glucose cotransporter SGLT1 in the small intestine (Kroiss et al., 2006; Chintalapati et al., 2016; Veyhl-Wichmann et al., 2016; Koepsell, 2017). RS1 mediates deceleration of the release of SGLT1-containing vesicles from the *trans*-Golgi network (TGN) (Supplemental Fig. 1). In the small intestine, uptake of D-glucose across the brush-border membrane (BBM) is rate limiting for glucose absorption (Gorboulev et al., 2012). Between meals when the glucose concentration in the small intestinal lumen and enterocytes is low, release of SGLT1-containing vesicles from the TGN is inhibited by RS1 fragments, which contain the regulatory domain RS1-Reg (Vernaleken et al., 2007; Veyhl-Wichmann et al., 2016).

Recently it was shown that RS1-Reg inhibits the enzymatic activity of ornithine decarboxylase (ODC) and that the inhibition of ODC promotes the release of SGLT1-containing vesicles from the TGN (Chintalapati et al., 2016). When the intracellular glucose concentration in enterocytes is increased after ingestion of glucose-rich food, glucose binds to ODC and abolishes the RS1-Reg-mediated inhibition of ODC activity. This promotes the release of SGLT1-containing vesicles from the TGN, which leads to a rapid increase of SGLT1 abundance in the BBM (see Supplemental Fig. 2, A and B). When phosphorylation of serine in a QSP (Gln-Ser-Pro) motif of

This study was funded by grants of the Deutsche Forschungsgemeinschaft [Grant SFB 487/C1 to H.K. and Grant GE2195/1-1] (to D.G.).
[1]D.G. and H.K. contributed equally to the work.
https://doi.org/10.1124/mol.118.113514.
[S] This article has supplemental material available at molpharm.aspetjournals.org.

ABBREVIATIONS: AMG, α-methyl-D-glucopyranoside; BBM, brush-border membrane; DFMO, difluoromethylornithine; GST, glutathione-*S*-transferase; hRS1, human RS1; hRS1-Reg, human RS1-Reg; hSGLT1, human SGLT1; hSGLT2, human SGLT2; hSGLT3, human SGLT3; MAP17, membrane-associated protein 17; MOPS, 3-(*N*-morpholino)propanesulfonic acid; ODC, ornithine decarboxylase; QEP, Gln-Glu-Pro; QSP, Gln-Ser-Pro; $QS_{SP}P$, QSP with thiophosphorylated serine; RS1-Reg, NH2-terminal regulatory domain of RS1; SGLT, Na^+-D-glucose cotransporter 1; SGLT2, Na^+-D-glucose cotransporter 2; SGLT3, D-glucose sensor; TGN, *trans*-Golgi network; YFP, yellow fluorescent protein.

human RS1-Reg (hRS1-Reg) was mimicked by introduction of a glutamate residue [hRS1-Reg(S20E)], the blunting effect of glucose on the down-regulation of SGLT1 at the TGN was abolished, resulting in down-regulation of the SGLT1-abundance in the BBM even under high glucose conditions (Chintalapati et al., 2016; Veyhl-Wichmann et al., 2016).

Decreasing glucose absorption in the small intestine by inhibition or down-regulation of SGLT1 in the BBM is a possibility to suppress the pathologic elevation of blood glucose in diabetes mellitus patients after uptake of glucose-containing food (Koepsell, 2017). Preclinical and clinical studies with orally administered SGLT1 inhibitors revealed a reduced elevation of plasma glucose levels and/or an increase of secretion of glucagon-like peptide 1 after ingestion of glucose-rich food (Shibazaki et al., 2012; Zambrowicz et al., 2012; Powell et al., 2013; Dobbins et al., 2015). Because SGLT1 is expressed in various organs, including the heart, lungs, and brain (Vrhovac et al., 2015), serious side effects are anticipated if SGLT1 inhibitors enter the blood (Connelly et al., 2018). Down-regulation of SGLT1 in the small intestinal BBM by oral application of peptides derived from hRS1-Reg that enter the enterocytes (Veyhl-Wichmann et al., 2016) may be a promising alternative to inhibition of SGLT1. It is easier to confine the effect of such peptides to enterocytes, particularly if peptide uptake into enterocytes is artificially enabled, such as by linkage to a membrane-permeating compound (Veyhl-Wichmann et al., 2016).

Previously we observed that peptides derived from RS1 in which phosphorylation was mimicked at selective positions, mediate either glucose-dependent posttranslational down-regulation of SGLT1 or glucose-independent down-regulation of the concentrative nucleoside transporter CNT1 (Veyhl-Wichmann et al., 2016). These data suggest diverse RS1-mediated posttranslational regulations of plasma membrane transporters, which must be considered during development of RS1-derived peptides for antidiabetic therapy.

In the present study we evaluated the possibilities and potential limitations of down-regulating SGLT1 in the small intestine by RS1-Reg–derived peptides after ingestion of glucose-rich food. We investigated whether the tripeptide motif QSP in hRS1-Reg, which enters enterocytes via the peptide transporter PEPT1 and down-regulates human SGLT1 (hSGLT1) in the presence of low but not of high intracellular glucose (Vernaleken et al., 2007), becomes effective at high intracellular glucose when serine is replaced by glutamate [Gln-Glu-Pro (QEP)], as has been observed after modification of QSP in hRS1-Reg [hRS1-Reg(S20E)] (Veyhl-Wichmann et al., 2016). Because this did prove to be the case, we determined in vitro whether SGLT1 in small intestinal mucosa can be down-regulated by extracellular application of QEP in presence of 5 mM D-glucose.

In addition, we investigated whether hRS1-Reg(S20E) and/or QEP are selective for hSGLT1 (*SLC5A1*) or also down-regulate the human Na^+-D-glucose cotransporter SGLT2 (hSGLT2) (*SLC5A2*), which is expressed in the kidney, and the human glucose sensor SGLT3 (hSGLT3) (*SLC5A4*), which is expressed in small intestine, kidney, brain, heart, skeletal muscle, and prostate (Diez-Sampedro et al., 2003; Wright et al., 2011). Our data show that hRS1-Reg(S20E) and QEP also down-regulate hSGLT2 and hSGLT3 and suggest that the same exocytotic pathway is addressed as in case of hSGLT1. At high glucose levels, SGLT1 in the small intestine is down-regulated after extracellular application of relatively high concentrations of QEP. Thus, QEP is proposed as antidiabetic drug using a formulation that improves uptake into enterocytes and prevents QEP exit into the blood.

Materials and Methods

Materials. α-methyl-D-[^{14}C]glucopyranoside ([^{14}C]AMG) (11.1 GBq/mmol) was obtained from American Labeled Chemical (St. Louis, MO) and D,L-[1-^{14}C]ornithine (2.07 TBq/mmol) from Hartmann Analytic (Braunschweig, Germany). Dulbecco's modified Eagle's medium (DMEM), DL-α-difluoromethylornithine (DFMO), and fetal calf serum were purchased from Sigma-Aldrich (Taufkirchen, Germany). We obtained penicillin/streptomycin solution from PAA Laboratories GmbH (Pasching, Austria) and tripeptides and QSP with thiophosphorylated serine ($QS_{SP}P$) from Xaia Custom Peptides (Göteborg, Sweden). Both hSGLT2 (gene *SLC5A2*) and MAP17 (product of gene *PDZK1IP1*) in vector pT7TS were kindly provided by Dr. Jean-Yves Lapointe from the University of Montreal, Centre-ville, Montréal, Québec, Canada (Coady et al., 2017). Other reagents were obtained as described elsewhere (Becker et al., 1996; Vernaleken et al., 2007).

Mice. Research was performed according to German law and our institutional guidelines. Mice were housed with free access to food and water ad libitum on a 12-hour light/dark cycle. Two- to 3-month-old C57BL6 wild-type mice and $RS1^{-/-}$ mice on C57BL6 background (Osswald et al., 2005) were used for the experiments. The mice were fed with standard chow (Ssniff V1534-000R/M-HND) obtained from Spezialdiäten GmbH (Soest, Germany). For ex vivo investigations performed at 11:00 and 12:00 AM, the animals were starved for 18 hours with free access to water.

Human Small Intestine. A 5-cm long fragment of the proximal jejunum, as routinely removed during a modification of Roux-en-Y gastric biliary bypass surgery (Cohen et al., 2006) of morbid obese patients (male and female, 40–60 years old) with a body mass index >35, was collected during surgeries. These tissues were added to ice-cold Dulbecco's modified Eagle's medium containing 10% (v/v) fetal calf serum, 1% (w/v) L-glutamine, 1% of a 1.5 mM penicillin/-streptomycin solution (PAA Laboratories GmbH), and 5 mM D-glucose. The uptake measurements were started 2 to 3 hours later. The usage of the human material was performed with written consent of patients and was approved by the ethic committee of the Medical Faculty of University of Würzburg.

Cloning. His-tagged hRS1-Reg mutants hRS1-Reg(S20A) and hRS1-Reg(S20E) were cloned in vector pET21a (Veyhl-Wichmann et al., 2016). Human RS1-Reg comprises amino acids 16–98 of hRS1. Yellow fluorescent protein (YFP) was fused to the C termini of hSGLT1 (YFP-hSGLT1) (Hediger et al., 1989), hSGLT2 (YFP-hSGLT2) (Coady et al., 2017), or hSGLT3 (YFP-hSGLT3) (Diez-Sampedro et al., 2003). Therefore, the complementary DNAs of hSGLT1, hSGLT2, or hSGLT3 were cloned into pGEM-derived USER-compatible oocyte expression vectors using an advanced uracil-excision-based cloning technique as described elsewhere (Nour-Eldin et al., 2006).

Expression and Purification of Ornithine Decarboxylase and hRS1-Reg Mutants. Expression and purification was performed as described elsewhere (Chintalapati et al., 2016). *Escherichia coli* bacteria (strain BL21Star; Live Technologies, Darmstadt, Germany) were transformed with plasmid pET42b encoding a fusion protein of glutathione-*S*-transferase (GST) with human ornithine decarboxylase 1 (hODC1) containing a thrombin cleavage site between the N-terminal GST-tag and hODC1 (GST-hODC1). GST-hODC1 was affinity-purified employing glutathione-sepharose 4B beads and was split with thrombin, and GST was removed. Purified hODC1 was dialyzed against 50 mM Tris-HCl, pH 7.2. We used pET21a plasmids containing His-tagged hRS1-Reg(S20A) or hRS1-Reg(S20E) for expression of the hRS1-Reg mutants in *E. coli* (strain BL21Star). The bacteria were lysed by sonication, cellular debris was removed by

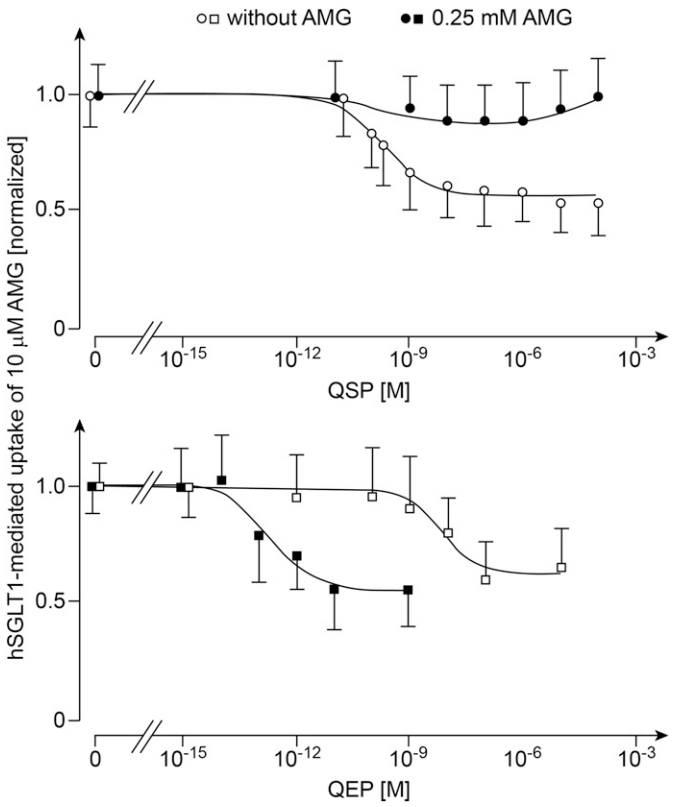

Fig. 1. Decrease of hSGLT1-mediated AMG uptake into oocytes after injection of tripeptides without or with coinjection of AMG. Oocytes were injected with hSGLT1-cRNA and incubated 2 days for expression. Thereafter oocytes were injected with potassium-rich buffer without AMG or with AMG that contained QSP or QEP. The concentration dependence of the down-regulation of hSGLT1-mediated AMG uptake by QSP (circles) or QEP (squares) in the absence and presence of coinjected AMG is shown. Mean values ± S.D. of 15–18 different cRNA injected oocytes are indicated. The oocytes were obtained from three different frogs. The measurements were normalized to the mean value for uptake in the absence of tripeptide. Curves showing inhibition were obtained by fitting the Hill equation to the compiled data sets.

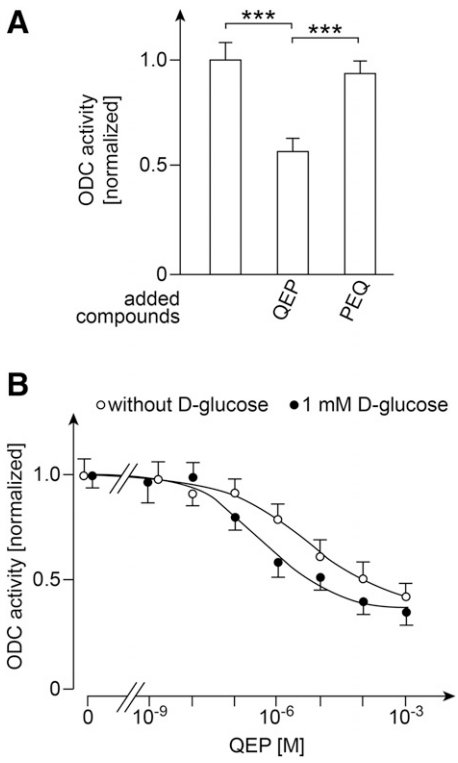

Fig. 2. Inhibition of enzymatic activity of hODC1 by QEP in the absence and presence of D-glucose. (A) Inhibition of enzymatic activity of purified hODC1 by 100 μM QEP versus 100 μM control peptide PEQ. (B) Concentration dependence of the inhibition of enzymatic activity of hODC1 by QEP in the absence or presence of 1 mM D-glucose. The measurements were performed by 1 hour of incubation at 37°C in the presence of 8 μM ornithine and 0.7 mM pyridoxal-5-phosphate. Mean values ± S.D. (n = 3) from three incubation assays using different preparations of hODC1 are shown. In each assay the enzymatic activity was determined by calculating the mean of triplicate measurements. The values were normalized to the mean value of ODC activity obtained in the absence of QEP and glucose. The indicated curves were obtained by fitting the Hill equation to the compiled data sets. ***$P <$ 0.001, analysis of variance with post hoc Tukey comparison.

centrifugation, and the His-tagged peptides were affinity-purified using nickel-charged agarose beads. The peptides were dialized against 5 mM 3-(*N*-morpholino)propanesulfonic acid (MOPS), pH 7.4, 103 mM KCl, and 1 mM $MgCl_2$. The purifications were monitored using SDS-PAGE and Western blotting (Chintalapati et al., 2016).

Measurement of Enzymatic Activity of hODC1. ODC activity was determined by measuring $^{14}CO_2$, which was liberated from L-[1-^{14}C]ornithine as described elsewhere (Chintalapati et al., 2016). The reaction was performed in closed vessels in which liberated $^{14}CO_2$ was trapped on filter papers that had been soaked with benzethonium hydroxide solution. We added 100 μl of 50 mM Tris-HCl pH 7.2 containing 0.81 μM pyridoxal-5-phosphate and 10 ng purified hODC1 plus different concentrations of tripeptide Gln-Glu-Pro (QEP) without or with 1.16 mM D-glucose to the vessels. To start the reaction we added 16 μl of 50 mM Tris–HCl, pH 7.2, containing 58 μM L-ornithine traced with ^{14}C-labeled L-ornithine, 2.5 mM dithiothreitol, and 0.1 mM EGTA, and the vessel was closed. After 1 hour of incubation at 37°C the reaction was stopped by adding 200 μl of 0.6 N perchloric acid. After an additional 30 minutes of incubation at 37°C, we analyzed the filter papers for radioactivity by liquid scintillation counting.

Measurements of the Effect of Tripeptides on AMG Uptake into Everted Small Intestinal Segments of Mice and into Human Small Intestinal Mucosa. For preparation of small intestinal segments, male mice were killed by cervical dislocation, and the small intestine was removed. After perfusion with Krebs-Ringer buffer (25 mM HEPES, pH 7.4, 108 mM NaCl, 4.8 mM KCl, 1.2 mM KH_2PO_4, and 1.2 mM $CaCl_2$), the small intestine was everted using a steel rod. Eight 1-cm long segments of the proximal jejunum were isolated, washed, and briefly stored in Krebs-Ringer buffer containing 5 mM D-glucose (Krebs-Ringer-glucose buffer).

For preparation of fragments of human small intestine, the intestinal segment obtained from bariatric surgery was opened and washed with Krebs-Ringer-glucose buffer. The mucosal layer was removed with fine scissors, and mucosal pieces with a surface area of 0.6 cm^2 were isolated using a punching instrument and were briefly stored in Krebs-Ringer-glucose buffer.

For preincubation of small intestinal samples, we incubated the small intestinal segments and mucosal pieces for 30 minutes at 37°C with Krebs-Ringer-glucose buffer in the absence (control) and presence of a tripeptide. Thereafter the intestinal samples were washed thoroughly with Krebs-Ringer buffer (room temperature).

For measurements of α-methyl-D-glucopyranoside (AMG) uptake, the samples were incubated for 2 minutes at 37°C with Krebs-Ringer buffer containing 10 μM [^{14}C]AMG. The incubations were performed in the absence of phlorizin or in the presence of 0.2 mM phlorizin. Uptake was stopped with ice-cold Krebs-Ringer buffer containing 0.2 mM phlorizin. The segments were washed with the same buffer, solubilized with Tissue Solubilizer, Soluene-350 (PerkinElmer, Waltham, MA), and their radioactivity was determined by liquid scintillation counting.

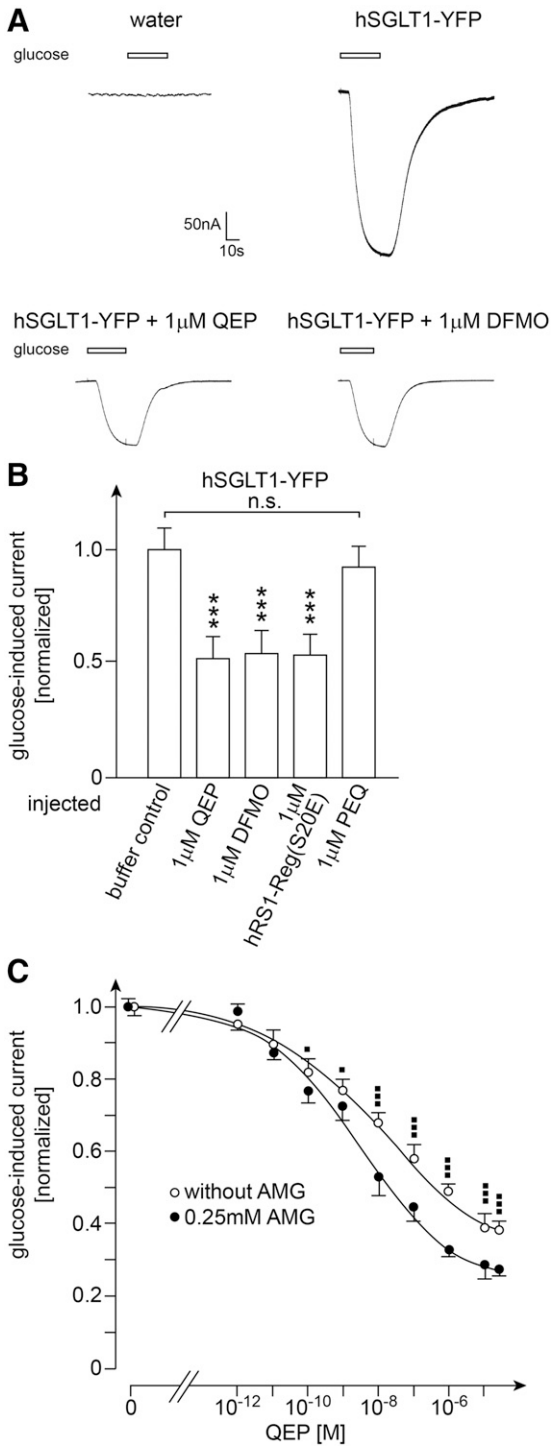

Fig. 3. Effects of injection of RS1-derived peptides, DFMO, and/or AMG into oocytes expressing hSGLT1-YFP on glucose-induced short-circuit currents. Oocytes were injected with water or cRNA of hSGLT1-YFP and incubated 4 or 5 days for expression. Thereafter the oocytes were injected with potassium-rich buffer without AMG (buffer control), without AMG plus indicated peptide or DFMO, or with AMG plus QEP. One hour later the oocytes were clamped to −50 mV, and the steady-state short-circuit inward currents were measured after superfusion with 100 mM D-glucose. (A) Original current traces recorded in the voltage clamp mode. (B) Effects of injection of different peptides or DFMO on glucose-induced short-circuit currents. (C) Effects of injection of various concentrations of QEP without or with coinjection of 0.25 mM AMG on glucose-induced short-circuit currents. (B and C) Mean values ± S.D. of 11–16 oocytes. The oocytes were obtained from three different frogs. Glucose-induced currents were normalized to the mean values of currents obtained after injection of potassium-rich buffer (buffer control). ***$P < 0.001$ analysis of variance with post hoc Tukey comparison, difference to buffer control; ■$P < 0.05$; ■■■$P < 0.001$ Student's t test for difference to value obtained after AMG coinjection. The indicated curves in C were obtained by fitting the Hill equation to the compiled data sets.

For each mouse and with each human small intestinal sample we performed uptake measurements after preincubation without and with tripeptide. [^{14}C]AMG uptake was measured in the absence or presence of phlorizin. Mean values of phlorizin inhibited uptake were calculated for each mouse or human small intestinal sample.

cRNA Synthesis. For cRNA synthesis, hSGLT1 in vector pBSII SK (Vernaleken et al., 2007), hSGLT1-YFP, hSGLT2-YFP, and hSGLT3-YFP in vector pNBI 22 (Nour-Eldin et al., 2006), and MAP17 in vector pT7TS (Coady et al., 2017) were used. To prepare sense cRNAs, the purified plasmids were linearized with EcoRI (hSGLT1, MAP17) or by polymerase chain reaction amplification of the vector region from the T7 promoter to the 3′UTR (hSGLT1-YFP, hSGLT2-YFP, hSGLT3-YFP). We synthesized m7Gppp[5′]-capped sense cRNAs using T3 polymerase (hSGLT1) or T7 polymerase (hSGLT1-YFP, hSGLT2-YFP, hSGLT3-YFP, MAP17) employing the mMESSAGE mMachine kit (Ambion Life Technologies, Austin, TX) (hSGLT1-cRNA) or the AmpliCap-Max T7 High Yield Message Maker Kid (Biozym Scientific GmbH, Hamburg, Germany).

Oocyte Preparation. Mature female *Xenopus laevis* frogs were anesthetized by immersion in water containing 0.1% 3-aminobenzoic acid ethyl ester. After a partial ovariectomy, stage V or VI oocytes were treated for 1.5 hours with 0.14 mg ml^{-1} collagenase I in Ca^{2+}-free ND96 buffer (10 mM HEPES, pH 7.4, 96 mM NaCl, 2 mM KCl, and 1 mM $MgCl_2$). Subsequently, the oocytes were washed with Ca^{2+}-free ND96 buffer and kept at 16°C in ND96 buffer (10 mM HEPES, pH 7.4, 96 mM NaCl, 2 mM KCl, 1 mM $MgCl_2$, and 1 mM $CaCl_2$) containing 50 mg/l gentamycin.

Heterologous Expression in Oocytes. Selected oocytes were injected with 50 nl of water or 50 nl of water containing the following cRNAs: 10 ng hSGLT1, 25 ng hSGLT1-YFP, 25 ng hSGLT2-YFP, 25 ng hSGLT3-YFP, 25 ng hSGLT2-YFP plus 10 ng MAP17. For measurements of hSGLT1-mediated AMG uptake, oocytes were incubated for 2 days after cRNA injection. For measurements of currents or membrane-associated fluorescence, cRNA-injected oocytes were incubated 4 to 5 days. Different incubation times were employed because the hSGLT1-mediated AMG uptake was well detectable but only very small glucose-induced currents were observed when the oocytes were incubated for only 2 days (see Supplemental Fig. 3). The oocytes were kept at 16°C in ND96 solution containing gentamycin. Water-injected control oocytes were incubated in parallel.

Injection of Peptides and Chemicals into Oocytes. One hour before measurements, hRS1-Reg, hRS1-Reg(S20E), hRS1-Reg(S20A), QSP, QEP, QSP with thiophosphorylated serine ($QS_{SP}P$), DFMO, and/or AMG were injected into the oocytes. We injected 50 nl of 5 mM MOPS, pH 7.4, 103 mM KCl, 1 mM $MgCl_2$ containing different amounts of peptides, 1.2 nmol DFMO, and/or 1.25 nmol AMG. The intracellular concentrations of the injected compounds were estimated by assuming an internal distribution volume of 0.4 μl (Zeuthen et al., 2002). The injected oocytes were maintained for 1 hour at room temperature in ND96 solution before measurements were started.

Measurement of AMG Uptake in Oocytes. We determined the hSGLT1-mediated AMG uptake by correcting the AMG uptake in hSGLT1-expressing oocytes for AMG uptake measured in non–cRNA-injected oocytes, which were handled in parallel (Veyhl-Wichmann et al., 2016). Oocytes were incubated for 20 minutes at room temperature in Ori buffer (5 mM HEPES, pH 7.6, 110 mM NaCl, 3 mM KCl, 1 mM $MgCl_2$, and 2 mM $CaCl_2$) containing 10 μM AMG traced with [^{14}C]AMG. Subsequently the oocytes were washed with ice-cold Ori buffer that contained 1 mM phlorizin. Individual oocytes

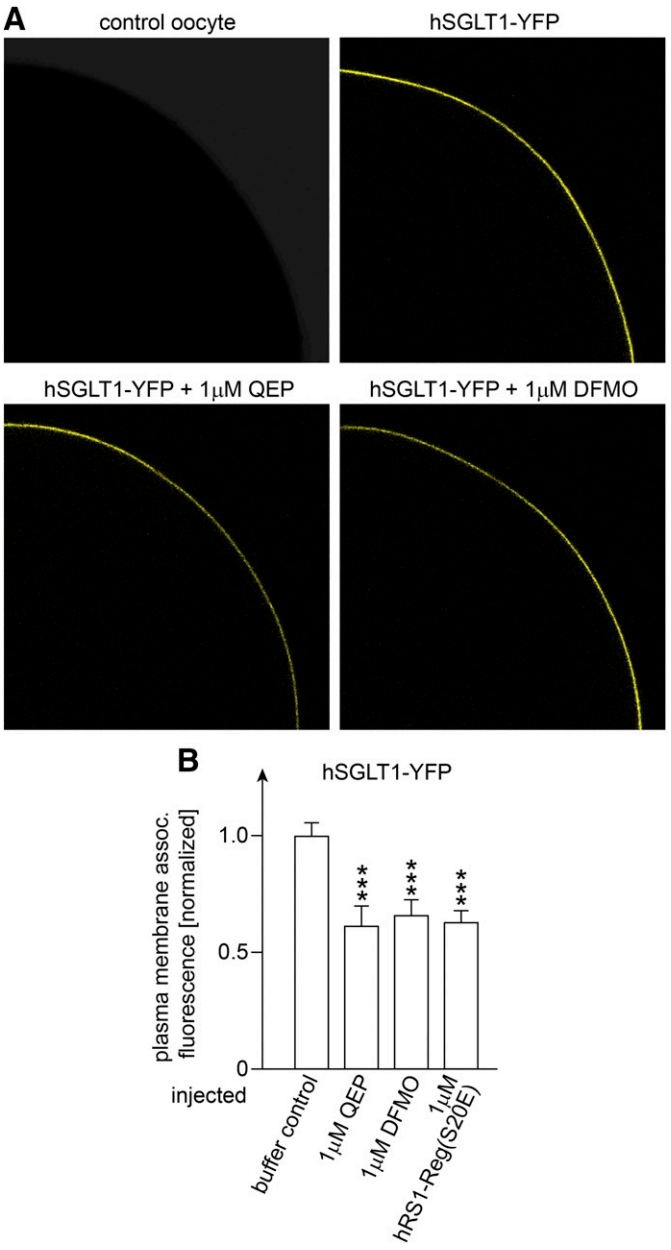

Fig. 4. Effects of injection of QEP, hRS1-Reg(S20E), or DFMO into oocytes expressing hSGLT1-YFP on plasma membrane-associated fluorescence. Oocytes were injected with water (A, control oocytes) or cRNA of hSGLT1-YFP and incubated 4 or 5 days for expression. Thereafter hSGLT1-YFP-expressing oocytes were injected with potassium-rich buffer [hSGLT1-YFP in (A), buffer control in (B)] or with potassium-rich buffer containing the compounds indicated in *B*. One hour later, YFP fluorescence associated with the plasma membrane of the oocytes was analyzed. (A) Representative confocal laser scanning images of oocytes. (B) Densitometric quantification of plasma membrane-associated YFP fluorescence intensity. Mean values ± S.D. of 9–12 oocytes from three different frogs are indicated. The values were normalized to the mean value of fluorescence measured after injection of potassium-rich buffer (buffer control). ***$P < 0.001$ for difference to buffer control, analysis of variance with post hoc Tukey comparison.

were solubilized in 5% (w/v) SDS and analyzed for radioactivity by scintillation counting.

Measurement of Glucose-Induced Short-Circuit Currents in Oocytes. Glucose-induced short-circuit currents of control oocytes (water-injected) and of oocytes expressing hSGLT1-YFP, hSGLT2-YFP, hSGLT2-YFP plus MAP17 or hSGLT3-YFP were measured with the double-electrode voltage clamp technique. The oocytes were superfused at room temperature in absence and presence of D-glucose at pH 5.0. The low pH was required to determine glucose-induced channel activity of hSGLT3 (Diez-Sampedro et al., 2003). The standard superfusion solution contained 10 mM 2-(*N*-morpholino)-ethanesulfonic acid (MES)/Tris buffer (pH 5.0), 30 mM Na-gluconate, 2 mM K-gluconate, 1 mM Mg-gluconate, 2 mM Ca-gluconate, and 165 mM sorbitol. The membrane potential was clamped to −50 mV, and the steady-state short-circuit current was measured continuously.

Glucose-induced steady-state short-circuit currents were measured by switching to a glucose-containing solution (based on the standard solution) in which 100 mM of sorbitol was replaced by 100 mM D-glucose. Glucose-induced currents were determined by subtracting the steady-state current in the absence of glucose from the steady-state current in the presence of 100 mM D-glucose. In water-injected control oocytes no significant glucose-induced currents were observed.

Tracing and Quantification of Fluorescence in Oocytes. We measured the YFP fluorescence intensity associated with the plasma membrane of oocytes expressing hSGLT1, hSGLT2, or hSGLT3 fused to YFP with a confocal laser-scanning microscope (Leica DM6000 CS; Leica Microsystems CMS GmbH, Mannheim, Germany) equipped with a Leica HCX IRAPO L25x/095W objective (excitation 514 nm, detection 528–580 nm). The optical plane was set to the equator of the oocyte, and the settings of YFP fluorescence acquisition (laser intensity and gain of photomultiplier tubes) were kept constant for all tested oocytes. YFP fluorescence intensity of a quarter circular segment per oocyte was measured using the LAS AF software from Leica.

Statistics and Fitting Procedures. The software package GraphPad Prism, version 4.1 (GraphPad Software, San Diego, CA) was used for analyses, with values expressed as mean ± S.D. For measurements of ODC activity, three incubation assays with triplicate determinations of enzymatic activities were performed using different preparations of hODC1.

To determine the hSGLT1-mediated glucose uptake in the small intestine, AMG uptake measurements in the absence and presence of phlorizin were performed, and the phlorizin-inhibited uptake was calculated. In the small intestine of each mouse two AMG uptake measurements in absence of phlorizin and two measurements in the presence of phlorizin were performed; in each human small intestinal sample four measurements without phlorizin and four measurements with phlorizin were conducted. The mean values ± S.D. of phlorizin-inhibited AMG uptake from three or more experiments with different mice or different preparations of human mucosa are reported.

For tracer uptake measurements in oocytes, the mean values ± S.D. were calculated from 15 to 18 oocytes. The oocytes were obtained from three different frogs. For electrical measurements and fluorescence measurements, the mean values ± S.D. were calculated from 9 to 16 individual oocytes, which were obtained from three or four different frogs.

The half-maximal concentration for inhibition (IC_{50}) and effective half-maximal concentration (EC_{50}) values for down-regulation were determined by fitting the Hill equation to the data considering the amount of remaining activity after maximal inhibition or down-regulation. The following equation was used, where v indicates the measured ODC activity or AMG uptake rate, x represents the logarithm of the tripeptide concentration, "top" indicates ODC activity in the absence of tripeptide or AMG uptake after preincubation without tripeptide, "bottom" indicates ODC activity of AMG uptake remaining after maximal inhibition or down-regulation, and n indicates the Hill coefficient. The maximally achieved down-regulation represents 1 – bottom.

$$v = \text{bottom} + (\text{top} - \text{bottom}) - \left(\frac{(\text{top} - \text{bottom}) \times (10^x)^n}{K_m{}^n + (10^x)^n}\right)$$

The K_m values for phlorizin-inhibited AMG uptake after preincubation without and with QEP were determined by fitting the Michaelis-Menten equation to the data. The presented curves were obtained by

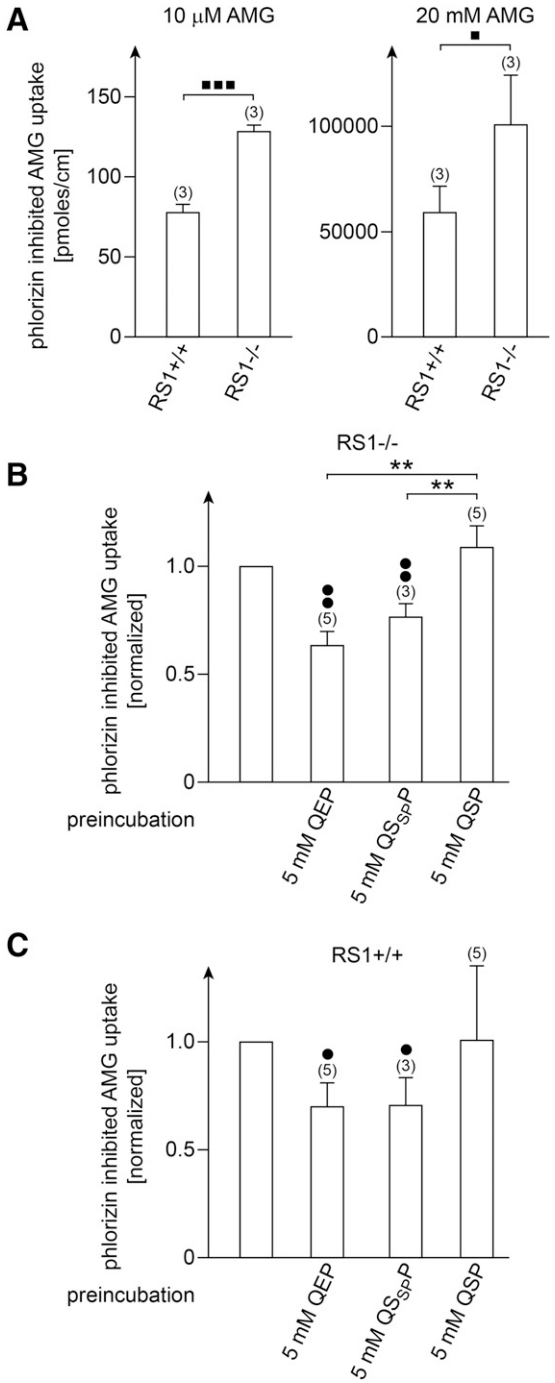

Fig. 5. Reduction of SGLT1-mediated glucose uptake in small intestinal mucosa of male RS1-knockout or male wild-type mice after preincubation with QEP or $QS_{SP}P$ in the presence of glucose. (A) Comparison of phlorizin-inhibited uptake of 10 μM or 20 mM AMG in small intestine of $RS1^{+/+}$ versus $RS1^{-/-}$ mice. One-centimeter long sections of everted jejunum were incubated with 10 μM AMG in the absence or presence of 0.2 mM phlorizin, and phlorizin-inhibited AMG uptake was determined. (B and C) Effects of preincubation of everted jejunum of male (B) $RS1^{-/-}$ mice or (C) $RS1^{+/+}$ mice with QEP, $QS_{SP}P$, or QSP. Segments of everted jejunal segments were incubated for 1 hour in the absence of tripeptides or in the presence of QEP, $QS_{SP}P$, or QSP. The incubations were performed in the presence of 5 mM D-glucose. Thereafter phlorizin-inhibited uptake of 10 μM AMG was measured. Measurements were normalized to AMG uptake in the same animal performed after incubation without tripeptide. Mean ± S.D. is indicated. The number of investigated animals is shown in parenthesis. $^{**}P < 0.01$, analysis of variance with post hoc Tukey comparison between the groups that were preincubated with QEP, $QS_{SP}P$, or QSP. $^{\blacksquare}P < 0.05$; $^{\blacksquare\blacksquare\blacksquare}P < 0.001$ Student's t test; $^{\bullet}P < 0.05$ difference to 1 is larger than 2 S.D. $^{\bullet\bullet}P < 0.01$ difference to 1 is larger than 3 S.D.

fitting the Hill or Michaelis-Menten equation to compiled data sets. The K_m values reported for the AMG concentration dependence of AMG uptake in human mucosa after preincubation without and with QEP (Fig. 6E) and the EC_{50} for QEP dependence of down-regulation of AMG uptake in human mucosa (Fig. 6D) were calculated by fitting the equations to the compiled data.

The EC_{50} values for concentration dependence of QEP-induced down-regulation in oocytes were obtained by fitting the Hill equation individually to each of three determinations that were performed with oocytes from different frogs. The IC_{50} value for inhibition of ODC activity by QEP was obtained by fitting the Hill equation to three individual incubation assays in which different preparations of hODC1 were employed. EC_{50} and IC_{50} values are presented as mean ± S.D. ($n = 3$). Hill coefficients were only presented for experiments in which the maximal down-regulation or inhibition was larger than 50%.

When more than two groups were compared, the statistical significance of differences was determined by one-way analysis of variance using post hoc Tukey comparison. Student's t test was used for the evaluation of statistical significance of differences between two groups. In experiments with small intestinal mucosa, where AMG uptake after preincubation with tripeptide was normalized to uptake after preincubation without tripeptide (Fig. 5, B and C; Fig. 6, B and C), the significance of the down-regulation of AMG uptake by tripeptide was evaluated considering whether the difference was larger than 2, 3, or 4 times the S.D. of uptake after preincubation with QEP.

Results

Down-Regulation of the ODC-Mediated Exocytotic Pathway of hSGLT1 by QEP in the Presence of High Intracellular Glucose. Previously we observed that the expression of hSGLT1-mediated AMG uptake in *Xenopus laevis* oocytes was decreased when the tripeptide QSP occurring two times in hRS1-Reg was injected (Vernaleken et al., 2007; Chintalapati et al., 2016). In oocytes expressing hSGLT1 the EC_{50} for down-regulation of AMG uptake by injected hRS1-Reg was increased when the oocytes were coinjected with 0.25 mM AMG whereas the EC_{50} for down-regulation of AMG uptake by hRS1-Reg(S20E) in which serine in a QSP motif was replaced by glutamate was decreased in the presence of 0.25 mM AMG (Veyhl-Wichmann et al., 2016).

We wondered whether the replacement of serine in the tripeptide QSP by glutamate would have a similar effect, so we compared the effect of 0.25 mM intracellular AMG on down-regulation of hSGLT1 by QSP versus QEP (Fig. 1). For down-regulation of hSGLT1 by QSP without coinjection of AMG, an EC_{50} value of 0.17 ± 0.04 nM ($n = 3$) was obtained whereas QSP concentrations up to 100 μM did not decrease AMG uptake in the presence of 0.25 mM intracellular AMG. Without injection of AMG, QEP decreased the hSGLT1-mediated AMG uptake maximally by 38% with an EC_{50} value of 10 ± 2.7 nM ($n = 3$). The EC_{50} value is 59 times higher compared with the EC_{50} value of QSP measured under the same conditions ($P < 0.001$); however, in the presence of 0.25 mM intracellular AMG, QEP decreased SGLT1-mediated AMG uptake by 46% with an EC_{50} value of 0.17 ± 0.10 pM

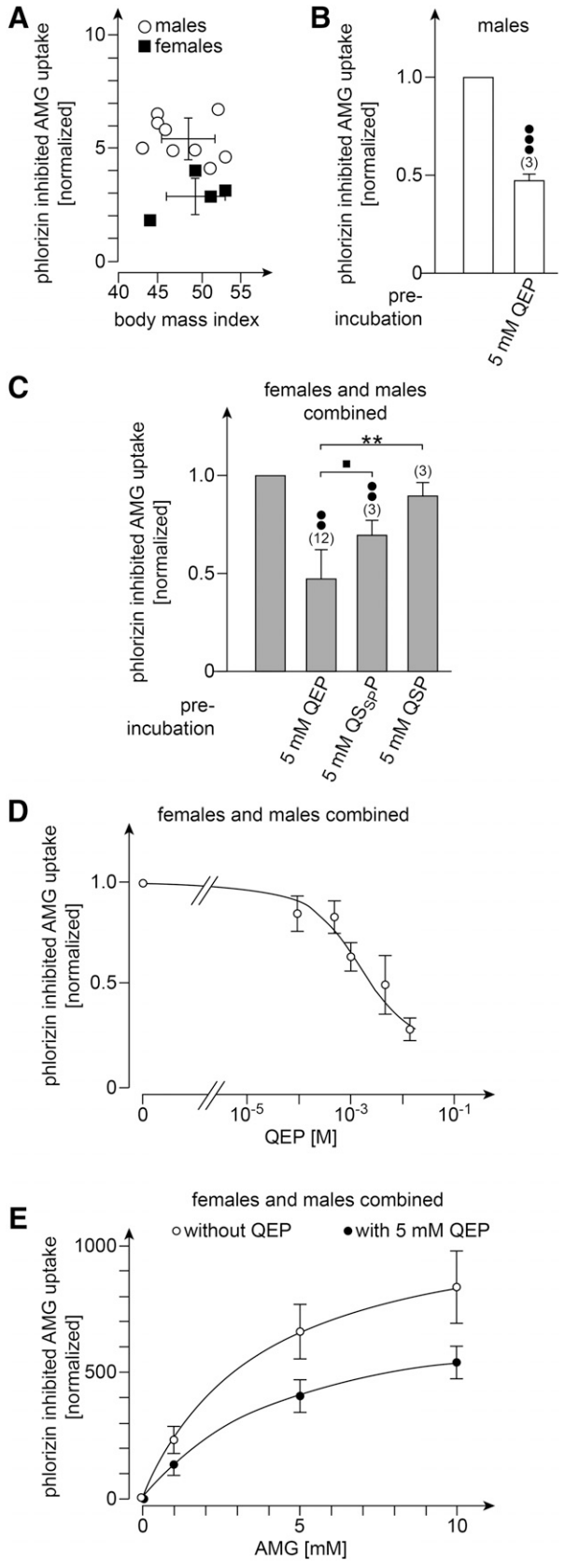

Fig. 6. Reduction of SGLT1-mediated glucose uptake into mucosa isolated from jejunum of morbidly obese patients after preincubation with QEP, $QS_{SP}P$, or QSP in the presence of glucose. (A) Comparison of phlorizin-inhibited uptake of 10 μM AMG into jejunal mucosa of female and male patients. The difference between phlorizin-inhibited AMG uptake measured in females versus males was statistically significant ($P < 0.001$). (B) Effect of incubation of jejunal mucosa of male patients with QEP. AMG uptake after incubation with QEP was normalized to AMG uptake after incubation without QEP observed in the same patient. (C) Effects of incubations of jejunal mucosa of patients with QEP, $QS_{SP}P$, or QSP on phlorizin-inhibited uptake of 10 μM AMG. Pieces of jejunal mucosa from female or male patients were incubated for 1 hour in the absence of tripeptide or in the presence of 5 mM QEP, $QS_{SP}P$ and QSP, and phlorizin-inhibited uptake of 10 μM AMG was measured. AMG uptake after incubation with peptide was normalized to AMG uptake after incubation without peptide observed in the same patient. (D) Reduction of phlorizin-inhibited AMG uptake observed after incubation of human jejunal mucosa with different concentrations of QEP. Pieces of jejunal mucosa from female or male patients were incubated with QEP and phlorizin-inhibited uptake of 10 μM AMG was measured. For each tested QEP concentration the inhibition of AMG uptake was determined in tissues from three patients, and the data were normalized to uptake of 10 μM AMG after incubation without QEP observed in the same patient. The curve was obtained by fitting the Hill equation to the data. (E) Substrate activation of AMG uptake into human jejunal mucosa of female and male patients measured after incubation without or with 5 mM QEP. For each AMG concentration uptake measurements were performed with tissue from three patients that had been preincubated in the absence or presence of QEP. Data were normalized to the phlorizin-inhibited uptake of 10 μM AMG into mucosa of the same patient that had been preincubated in the absence of QEP. Mean values ± S.D. are indicated. In *B* and *C* the numbers of investigated patients are given in parenthesis. In *D* the Hill equation and in *E* the Michaelis-Menten equation was fitted to the data. $^{**}P < 0.01$, analysis of variance with post hoc Tukey comparison between the groups that were preincubated with QEP, $QS_{SP}P$, and QSP; $^{\blacksquare}P < 0.05$ Student's *t* test; $^{\bullet\bullet}P < 0.01$ difference to 1 is larger than 3 S.D.; $^{\bullet\bullet\bullet}P < 0.001$ difference to 1 is larger than 4 S.D.

($n = 3$)—59,000-fold lower than without AMG injection ($P < 0.001$). The data indicate a high efficacy of QEP for post-translational down-regulation of hSGLT1-mediated transport in the presence of 0.25 mM intracellular AMG.

Previously we observed that the enzymatic activity of purified hODC1 was inhibited by 79% by hRS1-Reg(S20E), that the IC_{50} was decreased 3-fold in the presence of 1 mM D-glucose, and that the down-regulation of hSGLT1-mediated transport in oocytes by hRS1-Reg(S20E) and by the ODC inhibitor DFMO was not cumulative (Chintalapati et al., 2016). Based on these data we hypothesized that the down-regulation of the exocytotic pathway of SGLT1 by hRS1-Reg(S20E) is mediated via inhibition of ODC.

To verify that tripeptide QEP addresses the same pathway as hRS1-Reg(S20E), we investigated whether QEP also inhibits the enzymatic activity of purified hODC1 (Fig. 2). Comparing the enzymatic activity of purified hODC1 in the absence of tripeptides, in the presence of 0.1 mM QEP, or in the presence of 0.1 mM control peptide PEQ, we observed a 44% down-regulation by QEP (Fig. 2A).

In Fig. 2B we measured the effects of various QEP concentrations in absence or presence of 1 mM D-glucose. Fitting the Hill equation to the data, different IC_{50} values of 4.3 ± 1.7 and 0.43 ± 0.17 μM ($n = 3$, $P < 0.05$ for difference) were obtained in the absence or presence of D-glucose, respectively. This suggests that binding of D-glucose to hODC1 increases the efficacy of inhibition of hODC1 by QEP similar to inhibition by hRS1-Reg(S20E) (Chintalapati et al., 2016). In the absence or presence of glucose similar Hill coefficients of 0.47 ± 0.02 and 0.53 ± 0.15 were determined, indicating negative cooperativity between two inhibitory QEP binding sites at the functional hODC1 dimer that is not influenced by binding of D-glucose.

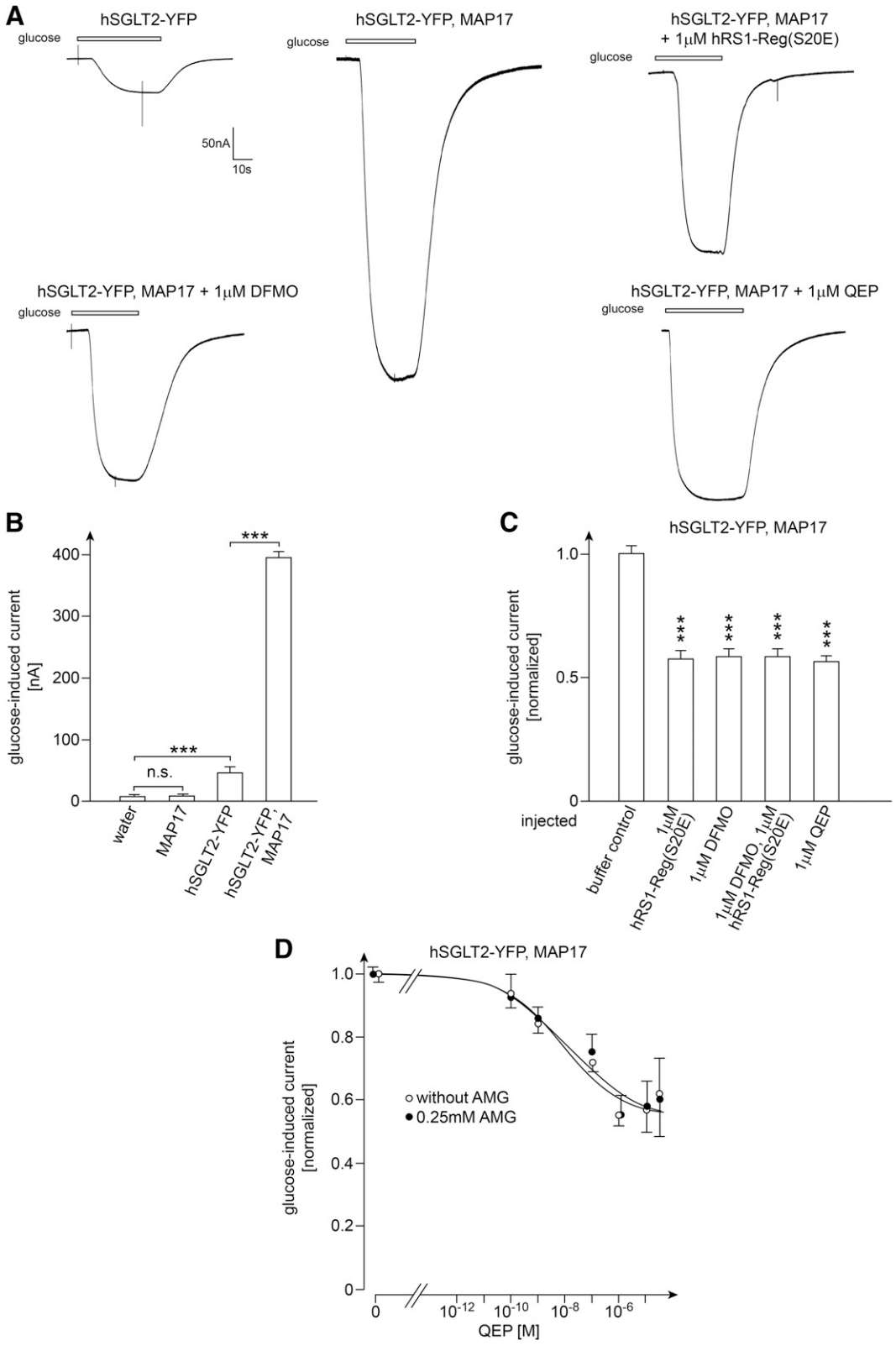

Fig. 7. Effects of injection of hRS1-Reg(S20E), DFMO, QEP, and/or AMG into oocytes expressing hSGLT2-YFP and MAP17 on glucose-induced short-circuit currents. Oocytes were injected with water, MAP17-cRNA, hSGLT2-YFP-cRNA, or cRNAs of MAP17 and hSGLT2-YFP and incubated 4 or 5 days for expression. The oocytes expressing hSGLT2-YFP plus MAP17 were injected with potassium-rich buffer (buffer control), potassium-rich buffer containing the indicated peptides and/or DFMO, or potassium-rich buffer containing AMG plus QEP. One hour later the oocytes were clamped to −50 mV, and steady-state, short-circuit inward currents were measured after superfusion with 100 mM D-glucose. (A) Original current traces. (B) Effect of

Next we investigated whether QEP and inhibition of ODC by DFMO down-regulate hSGLT1-mediated transport and abundance of hSGLT1 in the plasma membrane in parallel, as has been demonstrated for hRS1-Reg(S20E) (Chintalapati et al., 2016). We expressed hSGLT1 fused to YFP at its C terminus (hSGLT1-YFP) in oocytes and measured the effects of 1 μM QEP, 1 μM DFMO, or 1 μM hRS1-Reg(S20E) on 100 mM D-glucose-induced short-circuit inward currents at a holding potential −50 mV (Fig. 3, A and B) and on YFP fluorescence associated with the plasma membrane (Fig. 4, A and B).

One hour after injections of 1 μM QEP, 1 μM DFMO, or 1 μM hRS1-Reg(S20E) the glucose-induced short-circuit currents were reduced by about 50% compared with buffer-injected control oocytes (Fig. 3, A and B); the abundance of hSGLT1-YFP in the plasma membrane was decreased by about 40% (Fig. 4, A and B). After injection of 1 μM of the control peptide PEQ, no effect on the glucose-induced short-circuit current was observed (Fig. 3B). Similar effects of QEP, DFMO, and hRS1-Reg(S20E) on glucose-induced currents and YFP fluorescence at the plasma membrane suggest that QEP down-regulates hSGLT1 by inhibition of ODC, as has been proposed for hRS1-Reg(S20E) (Chintalapati et al., 2016).

Measuring the decrease of glucose-induced currents in hSGLT1-YFP–expressing oocytes after injection of various concentrations of QEP without or with coinjection of 0.25 mM AMG and fitting the Hill equation to the data, we determined EC_{50} values of 39 ± 8.8 and 3.8 ± 1.5 nM, respectively ($n = 3$, $P < 0.01$ for difference) (Fig. 3C). Maximal down-regulation by 77% ± 3% and 77% ± 5% was obtained and Hill coefficients of 0.25 ± 0.09 and 0.32 ± 0.05 were determined for the measurements performed without or with coinjection of AMG, respectively. In addition to similarities between the observed QEP effects on hSGLT1-mediated AMG uptake and hSGLT1-YFP mediated glucose-induced currents, distinct differences were obtained.

For AMG uptake a somewhat lower maximal down-regulation and an approximately 4-fold lower EC_{50} value were determined. Of note, in the uptake measurements the EC_{50} value was decreased 59,000-fold upon coinjection of AMG whereas in current measurements only a 10-fold decrease was observed. These differences may be explained by different regulatory states of the oocytes due to the different incubation times used for expression of hSGLT1 (2 days) versus hSGLT1-YFP (4 to 5 days).

Down-Regulation of SGLT1-Mediated AMG Uptake in Small Intestine of Mice and Humans by QEP in Presence of D-Glucose. To determine whether QEP is able to down-regulate SGLT1-mediated glucose uptake in small intestine after ingestion of glucose-rich food, we performed ex vivo uptake measurements in everted small intestinal segments of male mice and in pieces of human small intestinal mucosa. The pieces of human mucosa were isolated from jejunal segments that had been resected during bariatric surgery of morbid obese male and female patients. The everted murine intestinal segments and the human mucosal pieces were preincubated for 30 minutes at 37°C with QSP, QEP, or QSP in which serine was thiophosphorylated ($QS_{SP}P$). The preincubation was performed at 37°C in the presence of 108 mM sodium and 5 mM D-glucose trying to mimic luminal sodium and glucose concentrations after ingestion of glucose-rich food. Preincubation in the absence of glucose, resembling the situation between meals, was not performed because the mucosa disintegrated under this condition. After preincubation the samples were washed, and SGLT1-mediated phlorizin-inhibited uptake of 10 μM AMG was measured.

In mice the measurements were performed using jejunum from $RS1^{-/-}$ mice and wild-type mice. In mice without RS1, peptide effects could be observed independently from activity of endogenous RS1. In male $RS1^{-/-}$ mice the phlorizin-inhibited uptake of 10 μM or 20 mM AMG was about 70% higher compared with male wild-type mice (Fig. 5A). After preincubation of jejunum from male $RS1^{-/-}$ mice with 5 mM QEP or 5 mM $QS_{SP}P$, phlorizin-inhibited AMG uptake was decreased 37% and 22%, respectively, whereas no significant effect was observed after preincubation with QSP (Fig. 5B). Similar effects were observed with jejunum from male wild-type mice (Fig. 5C).

Human jejunal segments were obtained from 40- to 60-year-old morbid obese female and male patients. The phlorizin-inhibited uptake of 10 μM AMG into the mucosa per surface area was 2-fold higher in males compared with females (Fig. 6A). This effect was independent of the body mass index. The data suggest a higher abundance of hSGLT1 in the BBM of male obese versus female obese individuals. This was at variance with the observation that the abundance of hSGLT1 protein in the BBM of small intestine from normal weight individuals is similar between genders (Vrhovac et al., 2015). After incubation of mucosal pieces from male patients with 5 mM QEP in the presence of 5 mM D-glucose, the phlorizin-inhibited uptake of 10 μM AMG was about 50% decreased (Fig. 6B).

The same result was obtained with patients of mixed gender (Fig. 6C). Incubation of human small intestinal mucosa with 5 mM $QS_{SP}P$ resulted in about 30% inhibition of phlorizin-inhibited AMG uptake, whereas no effect was observed when the incubation was performed with 5 mM QSP. As shown in Fig. 6D, we determined the EC_{50} of QEP to inhibit phlorizin-inhibited uptake of 10 μM AMG into human mucosa of patients from mixed gender. An EC_{50} of 3.5 ± 2.9 mM was determined, suggesting that the rate-limiting step of the intracellular QEP effect is determined by the low affinity and turnover rate of the proton-peptide antiporter hPepT1 in the BBM, which is supposed to mediate the uptake of tripeptides (Liang et al., 1995; Vernaleken et al., 2007).

coexpression of MAP17 with hSGLT2-YFP on glucose induced short-circuit currents. The injected cRNA concentrations of MAP17 and hSGLT2-YFP were 10 and 25 ng, respectively. (C) Effects of injection of different peptides or DFMO on glucose-induced short-circuit currents in oocytes expressing hSGLT2-YFP and MAP17. (D) Effects of injection of various concentration of QEP without and with coinjection of 0.25 mM AMG on glucose-induced short-circuit currents in oocytes expressing hSGLT2-YFP and MAP17. (B–D) Mean values ± S.D. of 11–16 oocytes from three different frogs. (C and D) Glucose-induced currents normalized to the mean values of currents obtained after injection of potassium-rich buffer (buffer control). ***$P < 0.001$, analysis of variance with post hoc Tukey comparison. The indicated curves in *D* were obtained by fitting the Hill equation to the compiled data sets. Fitting the Hill equation separately to data obtained with oocytes from individual frogs, mean EC_{50} values ± S.D. ($n = 3$) of 33 ± 9 and 34 ± 10 nM were estimated for down-regulation without and with coinjection of AMG, respectively. n.s. no statistically significant difference.

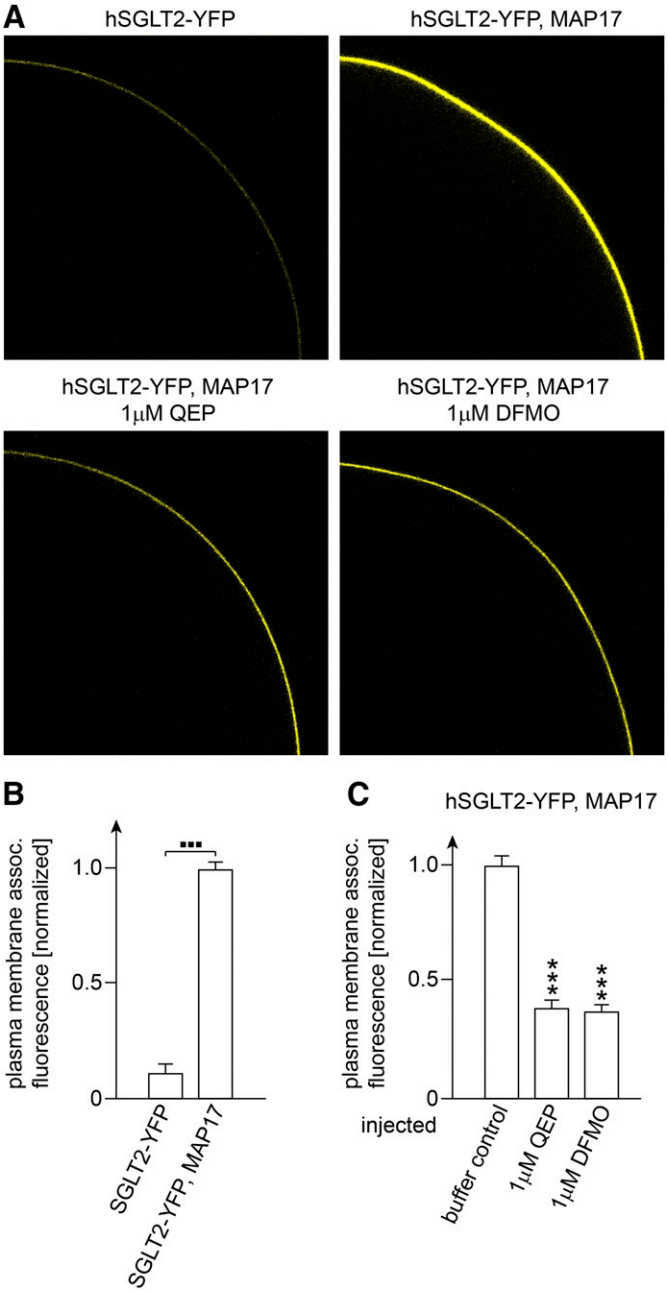

Fig. 8. Effects of coexpression of MAP17 with hSGLT2-YFP in oocytes on plasma membrane-associated fluorescence and effects of injection of QEP or DFMO into oocytes in which hSGLT2-YFP and MAP17 were coexpressed. Oocytes were injected with water, MAP17-cRNA, hSGLT2-YFP-cRNA, or cRNAs of hSGLT2-YFP and MAP17 and incubated 4 or 5 days for expression. Thereafter some oocytes were injected with potassium-rich buffer without addition (buffer control), with 1 μM QEP, or 1 μM DFMO. One hour later YFP fluorescence associated with the plasma membrane of the oocytes was analyzed by densitometry. (A) Typical fluorescence pictures. (B) Effect of coexpression of MAP17 on plasma membrane-associated fluorescence of hSGLT2-YFP. (C) Effect of injection of QEP or DFMO on plasma membrane-associated YFP fluorescence in oocytes expressing hSGLT2-YFP and MAP17. Expression and injection of QEP and DFMO were performed as in Fig. 7. Mean values ± S.D. of 9–12 oocytes are indicated. The oocytes were obtained from three different frogs. The plasma membrane-associated fluorescence was normalized to the mean value of fluorescence measured in oocytes expressing hSGLT2-YFP and MAP17 (B) or to the mean value of fluorescence measured in oocytes expressing hSGLT2-YFP and MAP17 which had been injected with potassium-rich buffer (buffer control). ***$P < 0.001$ for difference to buffer control, analysis of variance with post hoc Tukey comparison; ■■■$P < 0.001$ Student's t test.

In measuring the AMG-dependent activation of AMG uptake in human mucosa after preincubation in the absence or presence of AMG, we found similar apparent K_m values of 3.7 ± 1.0 and 4.6 ± 1.4 mM (Fig. 6E). This is consistent with the interpretation that QEP down-regulates the amount of hSGLT1 in the BBM without changing the functional properties of the transporter.

Posttranslational Down-Regulation of hSGLT2 Expressed in Oocytes by hRS1-Reg(S20E) and QEP. We wondered whether the ODC-mediated regulation of the exocytotic pathway of hSGLT1 by hRS1-Reg is selective for SGLT1 or also involves other members of the *SLC5* family such as hSGLT2 and hSGLT3. First, we investigated the effects of hRS1-Reg(S20E), QEP, and DFMO on glucose-induced short-circuit currents in oocytes expressing hSGLT2-YFP and MAP17. Four or 5 days after injection of hSGLT2-YFP alone, only very low glucose-induced short-circuit currents were observed; however, 8-fold higher glucose-induced currents were observed when the membrane-associated protein MAP17 was coexpressed, as has been described elsewhere (Coady et al., 2017) (Fig. 7, A and B).

MAP17 is a small membrane-associated protein located in the plasma membrane and Golgi (Kocher et al., 1996; Blasco et al., 2003). MAP17 contains a PDZ binding domain (acronym of the postsynaptic density protein PSD-95, the *Drosophila* junctional protein Disc-large, and the tight junctional protein ZO1) and serves as anchoring site for transporters such as multispecific organic anion transporter MRP2 (Kocher et al., 1999), the sodium-phosphate cotransporter NaPiIIa (Pribanic et al., 2003), and the sodium-proton exchanger NHE3 (Gisler et al., 2003). In addition, MAP17 induces reactive oxygen species, modulates intracellular signaling, and has been associated with tumor growth (Guijarro et al., 2007a,b). Whereas Coady et al. (2017) described that plasma membrane-associated immunoreactivity of C-terminal tagged hSGLT2 was not changed upon coexpression of MAP17, we observed a 9-fold increase of plasma membrane-associated immunofluorescence of hSGLT1-YFP (Fig. 8, A and B).

When 1 μM hRS1-Reg(S20E) was injected into oocytes expressing hSGLT2-YFP plus MAP17, the glucose-induced short-circuit currents measured 1 hour later were reduced by about 40% (Fig. 7C). A similar reduction of glucose-induced short-circuit currents was observed after injection of 1 μM DFMO or 1 μM hRS1(S20E) plus 1 μM DFMO. These data suggest that hRS1-Reg down-regulates the exocytotic pathway of hSGLT2 via inhibition of ODC activity as has been proposed for hSGLT1 (Chintalapati et al., 2016; Veyhl-Wichmann et al., 2016).

When 1 μM QEP was injected into oocytes expressing hSGLT2-YFP and MAP17, the same inhibitory effect on glucose-induced short-circuit currents was observed as after injection of hRS1-Reg(S20E) or DFMO (Fig. 7C). This supports the interpretation that QEP addresses the same ODC-dependent pathway of hSGLT2 as hRS1-Reg(S20E) as has been proposed for hSGLT1. To validate that the down-regulation of glucose-induced current observed after injection of QEP or DFMO is due to a decrease of hSGLT2-YFP abundance at the plasma membrane as observed for hSGLT1-YFP we also determined the effects of both compounds on plasma membrane-associated YFP (Fig. 8, A and C). An about 60% down-regulation of hSGLT2-YFP at the plasma membrane was observed.

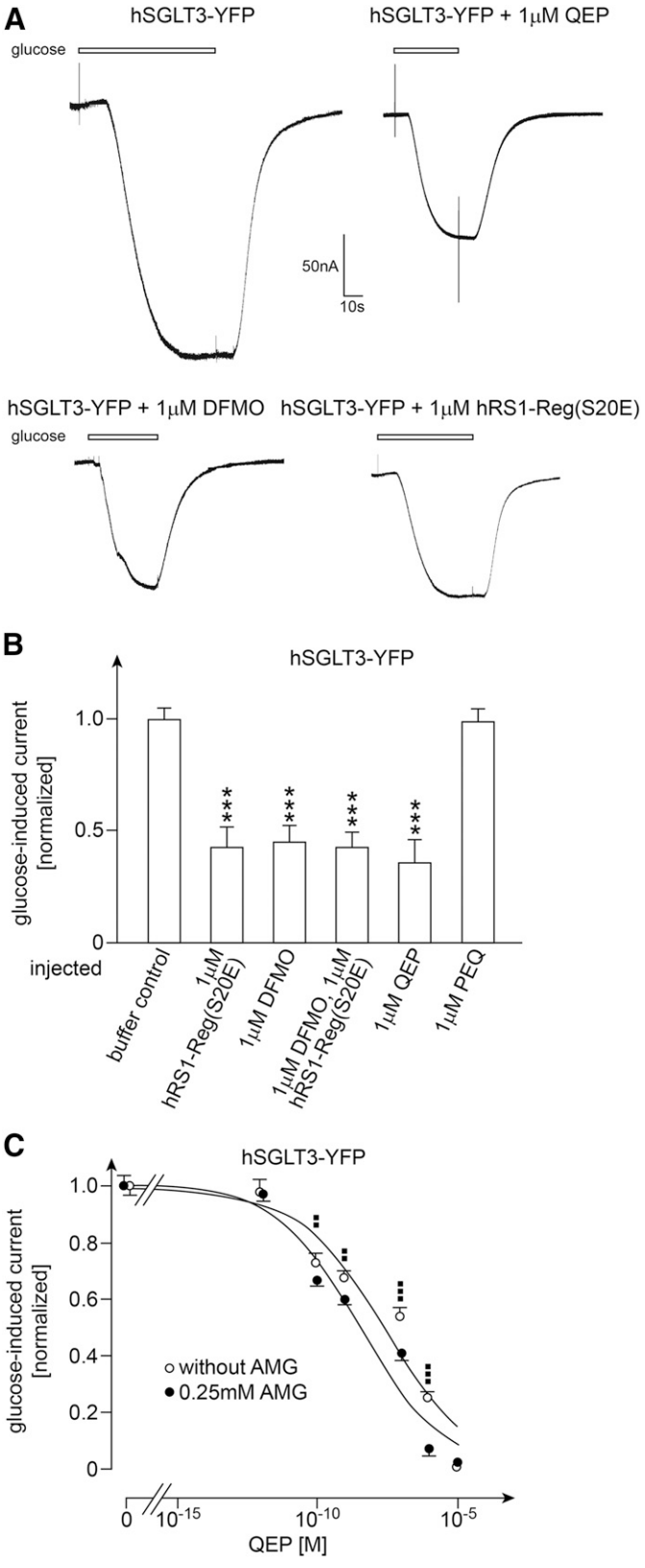

Fig. 9. Effects of injection of hRS1-Reg(S20E), DFMO, QEP, and/or AMG into oocytes expressing hSGLT3-YFP on glucose-induced short-circuit currents. Oocytes were injected with cRNA of hSGLT3-YFP and incubated 4 or 5 days for expression. Thereafter the oocytes were injected with potassium-rich buffer (buffer control), potassium-rich buffer containing the indicated peptides and/or DFMO, or potassium-rich buffer containing AMG plus QEP. One hour later the oocytes were clamped to −50 mV, and steady-state, short-circuit inward currents were measured after superfusion with 100 mM D-glucose. (A) Original current traces. (B) Effects of injection of different peptides, DFMO, or hRS1-Reg(S20E) plus DFMO on glucose-induced short-circuit currents. (C) Effects of injection of various concentrations of QEP without and with coinjection of 0.25 mM AMG on glucose-induced short-circuit currents. In *B* and *C* the mean values ± S.D. of 11–16 oocytes from three different frogs are indicated. Glucose-induced currents were normalized to the mean values of currents obtained after injection of potassium-rich buffer (buffer control). ***$P < 0.001$, analysis of variance with post hoc Tukey comparison for difference to buffer control; ■■$P < 0.01$; ■■■$P < 0.001$ Student's *t* test for difference to values obtained without and with coinjection of AMG. The indicated curves in *C* were obtained by fitting the Hill equation to the compiled data sets.

Measuring the down-regulation of glucose-induced current in oocytes expressing hSGLT2-YFP plus MAP17 after injection of various concentrations of QEP without or with coinjection of 0.25 mM AMG, we determined similar EC_{50} values of 10.0 ± 2.0 and 10.2 ± 7.7 nM, respectively ($n = 3$, each) (Fig. 7C). Without or with coinjection of AMG, maximal down-regulation by 52% ± 2.6% and 51% ± 4.9% was observed, and Hill coefficients of 0.35 ± 0.03 and 0.28 ± 0.07 were determined, respectively. The EC_{50} value in the absence of AMG was similar to the EC_{50} determined for down-regulation of hSGLT1-mediated AMG uptake whereas it is about 4 times lower compared with the EC_{50} value determined for hSGLT1-YFP-mediated glucose-induced currents. At variance with hSGLT1-mediated AMG uptake and hSGLT1-YFP-mediated currents, the EC_{50} for down-regulation of hSGLT2-YFP-mediated glucose-induced current by QEP was not altered after injection of AMG.

Posttranslational Down-Regulation of hSGLT3 Expressed in Oocytes by hRS1-Reg(S20E) and QEP. When oocytes were injected with hSGLT3-YFP and incubated for 4 to 5 days for expression, clamped to −50 mV, and superfused at pH 5.0 with 100 mM D-glucose, short-circuit currents of 120–150 nA were observed. One hour after injection of 1 μM hRS1(S20E), 1 μM DFMO, or 1 μM hRS1(S20E) plus 1 μM DFMO, the glucose-induced current was between 55% and 58% lower compared with oocytes in which buffer or 1 μM of the control peptide PEQ were injected (Fig. 9, A and B). After injection of 1 μM QEP, a 65% ± 2.6% reduction of glucose-induced short-circuit currents was observed, which was similar to the reduction observed after injection of 1 μM hRS1(S20E) or 1 μM DFMO (Fig. 9B).

For the effects of QEP and DFMO we showed that the decrease of glucose-induced current was associated with a 37%–39% decrease of membrane-associated fluorescence of hSGLT3-YFP (Fig. 10). In Fig. 9C we measured the concentration dependence of the QEP-mediated decrease of glucose-induced short-circuit current without and with injection of 0.25 mM AMG. In these experiments, injection of 1 μM QEP without and with coinjection of AMG reduced the glucose-induced currents by 72% ± 3% and 93% ± 3%, respectively ($n = 3$, $P < 0.001$ for difference). After injection of 10 μM QEP without and with coinjection of AMG, the glucose-induced currents were down-regulated almost completely.

Without and with coinjection of AMG, respective EC_{50} values of 33 ± 8.5 and 3.4 ± 0.7 nM were obtained ($n = 3$, $P < 0.01$ for difference), indicating that AMG increases the efficacy for down-regulation by QEP as observed for hSGLT1 and hSGLT1-YFP (Fig. 9C; Fig. 11B). For down-regulation of hSGLT3-YFP-mediated currents without and with coinjections of AMG, respective Hill coefficients of 0.30 ± 0.02 and 0.29 ± 0.02 were determined.

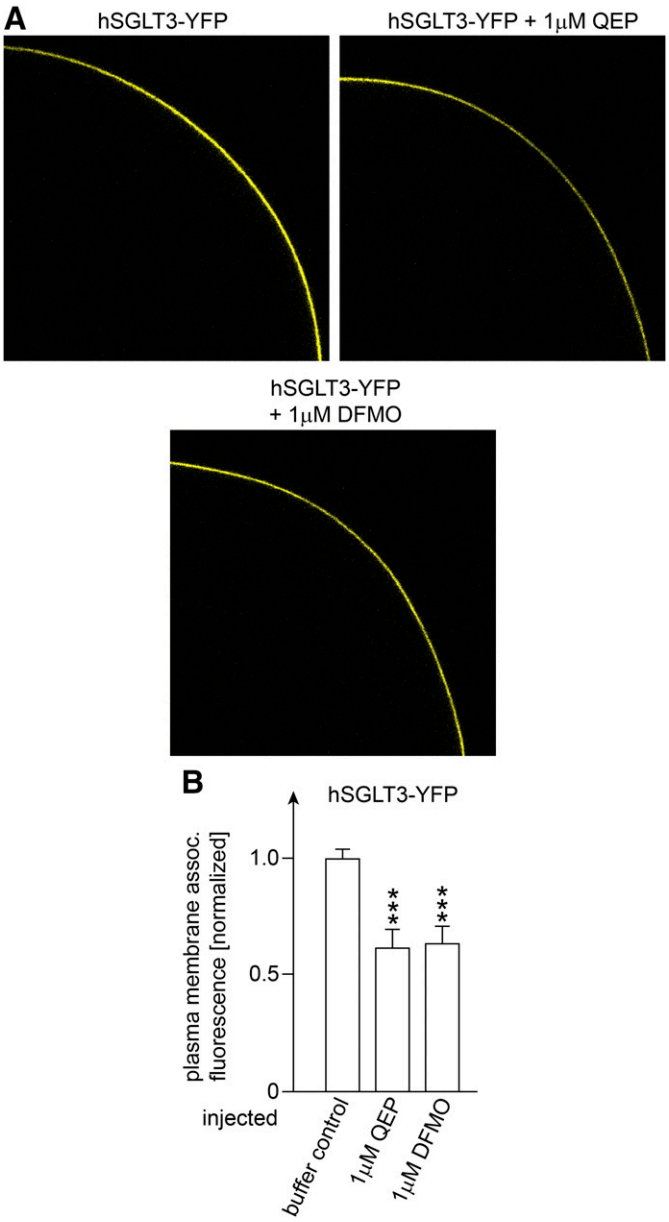

Fig. 10. Effects of injection of QEP or DFMO into oocytes expressing hSGLT3-YFP on plasma membrane-associated fluorescence of YFP. Oocytes were injected with cRNA of hSGLT3-YFP and incubated 4 or 5 days for expression. Thereafter the oocytes were injected with potassium-rich buffer without addition (buffer control), with 1 μM QEP, or with 1 μM DFMO. One hour later YFP fluorescence associated with the plasma membrane of the oocytes was analyzed. (A) Typical fluorescence pictures. (B) Effect of injection of QEP or DFMO on plasma membrane-associated YFP fluorescence. Mean values ± S.D. of 9–12 oocytes from three different frogs are indicated. The plasma membrane-associated fluorescence was normalized to the fluorescence measured in oocytes expressing hSGLT3-YFP which had been injected with potassium-rich buffer (buffer control). ***$P < 0.001$ for difference to buffer control, analysis of variance with post hoc Tukey comparison.

Discussion

We have provided evidence that QEP decreases the plasma membrane abundance and activity of hSGLT1 expressed in oocytes and SGLT1-mediated glucose transport in the small intestine in the presence of high glucose. Previously we had reported a similar effect for hRS1-Reg(S20E) in which serine in a QSP motif was replaced by glutamate mimicking phosphorylation (Veyhl-Wichmann et al., 2016). Our data suggest that QEP decelerates the exocytotic pathway of hSGLT1 like hRS1-Reg(S20E) by inhibiting ODC activity. Like hRS1-Reg(S20E), QEP inhibited the enzymatic activity of purified ODC; injection of QEP and ODC inhibitor DFMO into oocytes induced similar down-regulation of hSGLT1; and the IC_{50} value for inhibition of ODC by QEP was decreased in the presence of glucose.

Because RS1 and SGLT1 have been colocalized at the TGN (Korn et al., 2001) and antizyme inhibitor 2, which regulates vesicle trafficking via activation of ODC, has been also localized at the TGN (Parkkinen et al., 1997; Kanerva et al., 2010), we hypothesized that the posttranslational down-regulation of SGLT1 by hRS1-Reg(S20E) and QEP occurs at the TGN. Because glucose decreases the dissociation constant for binding of hRS1(S20E) to ODC and the IC_{50} values for inhibition of ODC by hRS1-Reg(S20E) or QEP (Chintalapati et al., 2016) (Fig. 2B), we presume that an allosteric effect of glucose binding to ODC on binding of hRS1-Reg(S20E) or QEP is involved in the glucose-induced efficacy increase observed for down-regulation of SGLT1 by these peptides (see the tentative model in Supplemental Fig. 2, A–D). However, because we observed largely different EC_{50} values for down-regulation of hSGLT1 and hSGLT1-YFP by QEP, additional factors are supposed to influence binding of hRS1-Reg and QEP to ODC.

It has been shown that phosphorylation of hRS1-Reg modulates the efficacy for down-regulation of hSGLT1 (Chintalapati et al., 2016; Veyhl-Wichmann et al., 2016), but this cannot explain the different EC_{50} values obtained for down-regulation of hSGLT1 and hSGLT1-YFP by QEP (see Fig. 11, A and B). We assume that different regulatory states of the employed oocytes that were incubated 2 days for expression of hSGLT1 and 4 to 5 days for expression of hSGLT1-YFP are involved. During incubation of the oocytes, the functional state of ODC may change due to changes in phosphorylation (Nemoto et al., 1984) and/or differential interaction of proteins such as antizymes and antizyme inhibitors that influence dimerization of ODC (Mangold and Leberer, 2005; Pegg, 2006).

Because dipeptides and tripeptides are transported by the proton-peptide cotransporter PepT1 into enterocytes (Daniel and Kottra, 2004; Vernaleken et al., 2007) we reasoned that orally applied QEP may down-regulate hSGLT1 after ingestion of glucose-rich food when posttranslational down-regulation of SGLT1 by endogenous RS1 is blunted (Veyhl-Wichmann et al., 2016). Performing in vitro measurements with everted small intestine of wild-type mice and with dissected mucosa from morbidly obese patients, we provided proof of principle that this is the case.

It has been shown that SGLT1-mediated uptake of glucose across the BBM is the rate-limiting step for small intestinal glucose absorption and that SGLT1 abundance in the BBM is up-regulated 4-fold in mice after gavage with glucose (Gorboulev et al., 2012). Hence, the observed 50% down-regulation of SGLT1-mediated glucose uptake across the BBM of small intestinal mucosa from morbidly obese patients by 5 mM QEP (Fig. 5C; Fig. 6, B and C) is supposed to decrease small intestinal glucose absorption substantially and to change glucose homeostasis. When measuring the concentration dependence of QEP added to the mucosal side of human

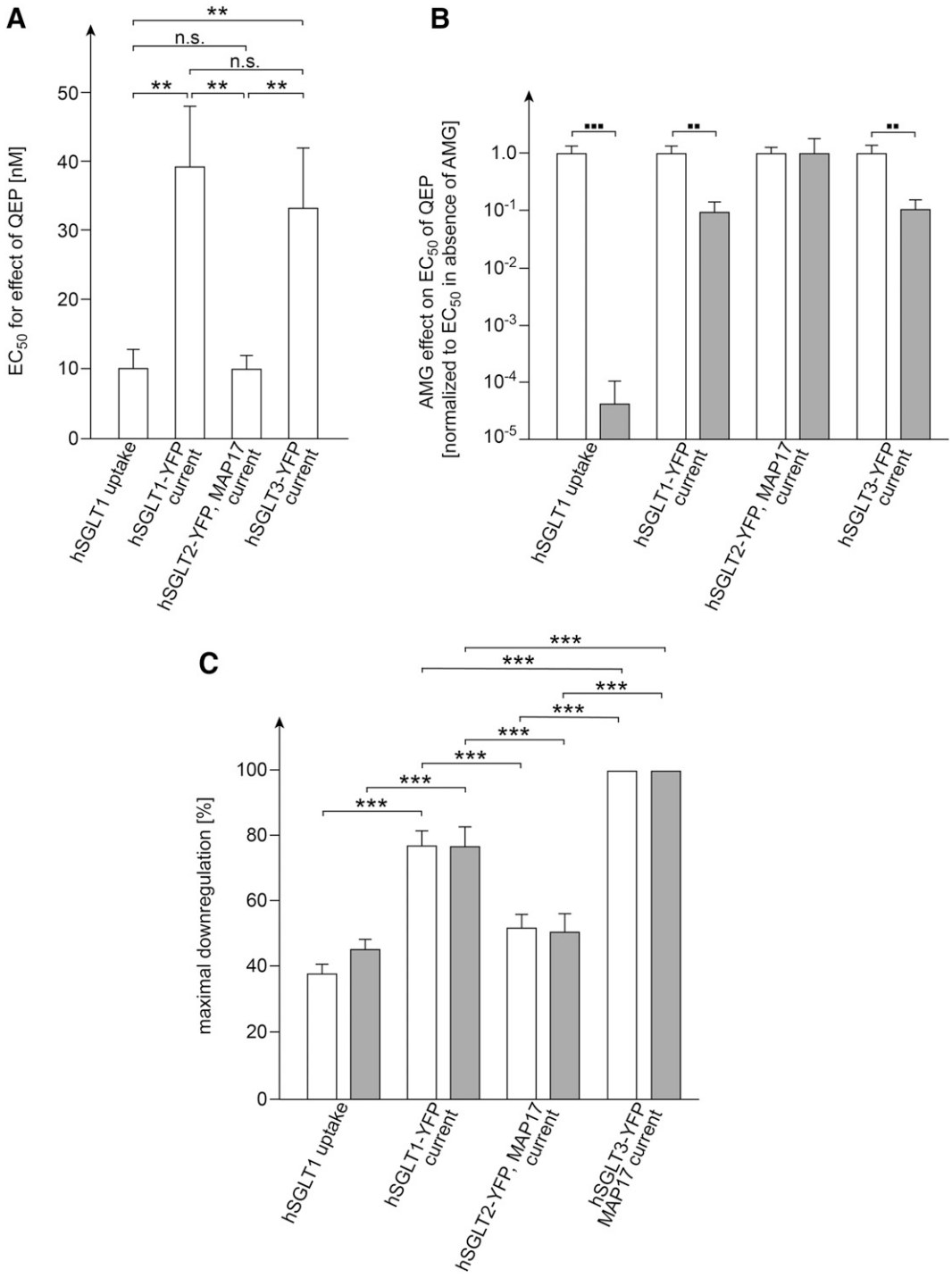

Fig. 11. Comparison of concentration-dependent QEP effects without and with coinjection of AMG on AMG uptake in oocytes expressing hSGLT1 and glucose-induced currents in oocytes expressing hSGLT1-YFP, hSGLT2-YFP plus MAP17, or hSGLT3-YFP. The indicated values are derived from data shown in Fig. 1, Fig. 3C, Fig. 7D, and Fig. 9C. For each condition the Hill equation was fitted to three experiments performed with oocytes from one individual frog. Mean values ± S.D. are indicated. Open columns represent measurements without coinjection of AMG, closed columns represent measurements with coinjection of AMG. (A) EC_{50} values of effects obtained after injection of QEP without coinjection of AMG. (B) Effects of coinjection of 0.25 mM AMG on EC_{50} values determined for down-regulation of transport activities by QEP. The data were normalized to the mean value of the respective EC_{50} value obtained without coinjection of AMG shown in (A). (C) Maximally obtained down-regulation (see *Materials and Methods*). $^{**}P < 0.01$; $^{***}P < 0.001$; n.s. no statistically significant difference analysis of variance with post hoc Tukey comparison; $^{■■}P < 0.01$; $^{■■■}P < 0.001$ Student's *t* test.

small intestinal mucosa to down-regulate SGLT1-mediated AMG uptake, we determined an EC_{50} value of 3.5 ± 4.9 mM.

Considering that the EC_{50} values determined for the intracellular concentration of QEP required for down-regulation of hSGLT1 in oocytes are at least 10,000 times lower, it is evident that the uptake of QEP into enterocytes is insufficient and that an oral application of mere QEP is not suitable for therapy. Of note, we observed a 50% down-regulation of hSGLT1-mediated glucose transport when human Caco-2 cells were incubated for 30 minutes with 0.03 nM hRS1-Reg(S20E)

linked to nanohydrogel (Chintalapati et al., 2016). Thus, coupling of small peptides containing the QEP motif to nanohydrogels may be a promising alternative for oral treatment with QEP.

To try to evaluate potential risks of down-regulation of SGLT1 in small intestine by QEP or QEP containing peptides, we investigated the selectivity of hRS1-Reg(S20E) and QEP. Previously we had observed that hRS1-Reg down-regulates SGLT1 in a glucose-dependent manner via inhibition of ODC whereas it down-regulates the concentrative nucleoside transporter CNT1 independently of glucose and ODC, and that phosphorylation of RS1-Reg has differential impact on both regulations (Veyhl-Wichmann et al., 2016). Our present data indicate that, in addition to hSGLT1, hSGLT2 and hSGLT3 also are down-regulated by hRS1-Reg(S20E) and QEP. This suggests that an inhibition of ODC by hRS1(S20E) and QEP is involved. At variance to CNT1, the transport activity and plasma membrane abundance of hSGLT2-YFP and hSGLT3-YFP in oocytes were down-regulated by inhibition of ODC with 1 μM DFMO. In addition, the decreases of glucose-induced currents induced by 1 μM hRS1-Reg(S20E) plus 1 μM DFMO were not cumulative as observed for hSGLT1 (Chintalapati et al., 2016).

Concerning dose–response effects of QEP for down-regulation of glucose-induced currents mediated by hSGLT1-YFP, hSGLT2-YFP, or hSGLT3-YFP, we observed similarities but also distinct differences. Thus, without coinjection of AMG similar EC_{50} values have been obtained for hSGLT1-YFP and hSGLT3-YFP, but the EC_{50} for hSGLT2-YFP was 4-fold smaller (Fig. 11A). Similarly, coinjection of AMG induced a 10-fold decrease of the EC_{50} value of glucose-induced currents mediated by hSGLT1-YFP or hSGLT3-YFP, but it did not change the EC_{50} for hSGLT2-YFP (Fig. 11B). For QEP-mediated down-regulation of glucose-induced currents by hSGLT1-YFP and hSGLT3-YFP, we determined similar Hill coefficients of 0.25 and 0.30, indicating negative cooperativity.

The differences between efficacy and AMG dependence of QEP for down-regulation of hSGLT2-YFP-mediated, glucose-induced current versus glucose-induced currents by hSGLT1-YFP or hSGLT3-YFP are probably due to a regulatory effect due to the coinjection of MAP17 with hSGLT2-YFP, which we performed to obtain sufficiently high functional activity of this transporter in oocytes (see the tentative model in Supplemental Fig. 2, C–F). MAP17 is a multifunctional protein that has been located to the plasma membrane and the Golgi (Blasco et al., 2003). It has been also shown to promote clustering of transporters and to activate reactive oxygen species–associated signaling cascades (Gisler et al., 2003; Guijarro et al., 2007b).

Our observation that the abundance of hSGLT2-YFP at the plasma membrane was increased after coexpression of MAP17 suggests an involvement of MAP17 in posttranscriptional regulation. The observed differences in QEP efficacy and glucose-dependence of QEP efficacy of hSGLT2-YFP versus hSGLT1-YFP and hSGLT3-YFP expressed without MAP17 point to an involvement of MAP17 in the RS1-Reg–mediated regulation of hSGLT2 at the Golgi.

For glucose-induced currents mediated by hSGLT1-YFP, hSGLT2-YFP, and hSGLT3-YFP, we observed different degrees of maximal down-regulation by QEP (Fig. 11C). This was expected because transporter plasma membrane abundance in response to the hypothesized QEP-mediated down-regulation of vesicle release from the TGN is supposed to be influenced by a scenario of processes, which are expected to differ between the three transporters (see scheme in Supplemental Fig. 1). The involved processes include transporter delivery to the TGN, cleavage of transporter containing vesicles from the TGN, exocytosis, endocytosis, and transporter degradation.

SGLT2 and SGLT1 have been identified as targets for the treatments of diabetes and cancer (Koepsell, 2017). Drugs have been developed that inhibit functional activity of hSGLT2 or hSGLT1, but cross-inhibition with hSGLT3, which is involved in glucose-dependent neuronal regulations of food intake, has yet to be evaluated (Koepsell, 2017). Drugs that address the posttranslational regulation of SGLT1 or SGLT2 represent a promising alternative to inhibitors because they may promote more prolonged effects compared with inhibitors. The complex posttranslational regulations of hSGLT1-3 are poorly understood, but some involved proteins such as RS1 and MAP17 have been identified. The observation that a modified tripeptide motif of hRS1 (QEP) down-regulates SGLT1 after ingestion of glucose-rich food has opened the exciting possibility of down-regulating small intestinal glucose absorption. The observation that QEP also regulates hSGLT2 expressed in the kidney and hSGLT3 expressed in the portal vein, muscle, and brain indicates that QEP-based drugs must be developed that allow a selective application of QEP to enterocytes.

Acknowledgments

We thank Dr. Jean-Yves Lapointe from the Physics Department of University of Montreal, Montreal, Quebec, Canada for supplying the cDNA of hSGLT1 and the vector pT7TS containing MAP17. We also thank Michael Christof from the Institute of Anatomy and Cell Biology of the University of Würzburg for generating the figures.

Authorship Contributions

Participated in research design: Schäfer, Geiger, Koepsell.

Conducted experiments: Schäfer, Rikkala, Veyhl-Wichmann, Keller.

Contributed new reagents or analytic tools: Jurowich, Geiger, Koepsell.

Performed data analysis: Schäfer, Rikkala, Veyhl-Wichmann, Keller, Geiger, Koepsell.

Wrote or contributed to the writing of the manuscript: Koepsell.

References

Becker D, Dreyer I, Hoth S, Reid JD, Busch H, Lehnen M, Palme K, and Hedrich R (1996) Changes in voltage activation, Cs^+ sensitivity, and ion permeability in H5 mutants of the plant K^+ channel KAT1. *Proc Natl Acad Sci USA* **93**:8123–8128.

Blasco T, Aramayona JJ, Alcalde AI, Catalán J, Sarasa M, and Sorribas V (2003) Rat kidney MAP17 induces cotransport of Na-mannose and Na-glucose in *Xenopus laevis* oocytes. *Am J Physiol Renal Physiol* **285**:F799–F810.

Chintalapati C, Keller T, Mueller TD, Gorboulev V, Schäfer N, Zilkowski I, Veyhl-Wichmann M, Geiger D, Groll J, and Koepsell H (2016) Protein RS1 (RSC1A1) downregulates the exocytotic pathway of glucose transporter SGLT1 at low intracellular glucose via inhibition of ornithine decarboxylase. *Mol Pharmacol* **90**: 508–521.

Coady MJ, El Tarazi A, Santer R, Bissonnette P, Sasseville LJ, Calado J, Lussier Y, Dumayne C, Bichet DG, and Lapointe JY (2017) MAP17 is a necessary activator of renal Na^+/glucose cotransporter SGLT2. *J Am Soc Nephrol* **28**:85–93.

Cohen R, Pinheiro JS, Correa JL, and Schiavon CA (2006) Laparoscopic Roux-en-Y gastric bypass for BMI $<$ 35 kg/m^2: a tailored approach. *Surg Obes Relat Dis* **2**: 401–404, discussion 404.

Connelly KA, Zhang Y, Desjardins J-F, Thai K, and Gilbert RE (2018) Dual inhibition of sodium-glucose linked cotransporters 1 and 2 exacerbates cardiac dysfunction following experimental myocardial infarction. *Cardiovasc Diabetol* **17**:99.

Daniel H and Kottra G (2004) The proton oligopeptide cotransporter family SLC15 in physiology and pharmacology. *Pflugers Arch* **447**:610–618.

Diez-Sampedro A, Hirayama BA, Osswald C, Gorboulev V, Baumgarten K, Volk C, Wright EM, and Koepsell H (2003) A glucose sensor hiding in a family of transporters. *Proc Natl Acad Sci USA* **100**:11753–11758.

Dobbins RL, Greenway FL, Chen L, Liu Y, Breed SL, Andrews SM, Wald JA, Walker A, and Smith CD (2015) Selective sodium-dependent glucose transporter

1 inhibitors block glucose absorption and impair glucose-dependent insulinotropic peptide release. *Am J Physiol Gastrointest Liver Physiol* **308**:G946–G954.
Gisler SM, Pribanic S, Bacic D, Forrer P, Gantenbein A, Sabourin LA, Tsuji A, Zhao Z-S, Manser E, Biber J, et al. (2003) PDZK1: I. a major scaffolder in brush borders of proximal tubular cells. *Kidney Int* **64**:1733–1745.
Gorboulev V, Schürmann A, Vallon V, Kipp H, Jaschke A, Klessen D, Friedrich A, Scherneck S, Rieg T, Cunard R, et al. (2012) Na^+-D-glucose cotransporter SGLT1 is pivotal for intestinal glucose absorption and glucose-dependent incretin secretion. *Diabetes* **61**:187–196.
Guijarro MV, Leal JF, Blanco-Aparicio C, Alonso S, Fominaya J, Lleonart M, Castellvi J, Ramon y Cajal S, and Carnero A (2007a) MAP17 enhances the malignant behavior of tumor cells through ROS increase. *Carcinogenesis* **28**: 2096–2104.
Guijarro MV, Link W, Rosado A, Leal JF, and Carnero A (2007b) MAP17 inhibits Myc-induced apoptosis through PI3K/AKT pathway activation. *Carcinogenesis* **28**: 2443–2450.
Hediger MA, Turk E, and Wright EM (1989) Homology of the human intestinal Na^+/glucose and *Escherichia coli* Na^+/proline cotransporters. *Proc Natl Acad Sci USA* **86**: 5748–5752.
Kanerva K, Mäkitie LT, Bäck N, and Andersson LC (2010) Ornithine decarboxylase antizyme inhibitor 2 regulates intracellular vesicle trafficking. *Exp Cell Res* **316**: 1896–1906.
Kocher O, Cheresh P, and Lee SW (1996) Identification and partial characterization of a novel membrane-associated protein (MAP17) up-regulated in human carcinomas and modulating cell replication and tumor growth. *Am J Pathol* **149**: 493–500.
Kocher O, Comella N, Gilchrist A, Pal R, Tognazzi K, Brown LF, and Knoll JH (1999) PDZK1, a novel PDZ domain-containing protein up-regulated in carcinomas and mapped to chromosome 1q21, interacts with cMOAT (MRP2), the multidrug resistance-associated protein. *Lab Invest* **79**:1161–1170.
Koepsell H (2017) The Na^+-D-glucose cotransporters SGLT1 and SGLT2 are targets for the treatment of diabetes and cancer. *Pharmacol Ther* **170**:148–165.
Korn T, Kühlkamp T, Track C, Schatz I, Baumgarten K, Gorboulev V, and Koepsell H (2001) The plasma membrane-associated protein RS1 decreases transcription of the transporter SGLT1 in confluent LLC-PK_1 cells. *J Biol Chem* **276**:45330–45340.
Kroiss M, Leyerer M, Gorboulev V, Kühlkamp T, Kipp H, and Koepsell H (2006) Transporter regulator RS1 *(RSC1A1)* coats the *trans*-Golgi network and migrates into the nucleus. *Am J Physiol Renal Physiol* **291**:F1201–F1212.
Liang R, Fei Y-J, Prasad PD, Ramamoorthy S, Han H, Yang-Feng TL, Hediger MA, Ganapathy V, and Leibach FH (1995) Human intestinal H^+/peptide cotransporter. Cloning, functional expression, and chromosomal localization. *J Biol Chem* **270**: 6456–6463.
Mangold U and Leberer E (2005) Regulation of all members of the antizyme family by antizyme inhibitor. *Biochem J* **385**:21–28.
Nemoto O, Aoyagi T, and Miura Y (1984) Ornithine decarboxylase activity is inhibited by epidermal polyamine-dependent protein kinase-mediated phosphorylation. *J Invest Dermatol* **83**:257–260.
Nour-Eldin HH, Hansen BG, Nørholm MH, Jensen JK, and Halkier BA (2006) Advancing uracil-excision based cloning towards an ideal technique for cloning PCR fragments. *Nucleic Acids Res* **34**:e122.
Osswald C, Baumgarten K, Stümpel F, Gorboulev V, Akimjanova M, Knobeloch K-P, Horak I, Kluge R, Joost H-G, and Koepsell H (2005) Mice without the regulator gene *Rsc1A1* exhibit increased Na^+-D-glucose cotransport in small intestine and develop obesity. *Mol Cell Biol* **25**:78–87.
Parkkinen JJ, Lammi MJ, Agren U, Tammi M, Keinänen TA, Hyvönen T, and Eloranta TO (1997) Polyamine-dependent alterations in the structure of microfilaments, Golgi apparatus, endoplasmic reticulum, and proteoglycan synthesis in BHK cells. *J Cell Biochem* **66**:165–174.
Pegg AE (2006) Regulation of ornithine decarboxylase. *J Biol Chem* **281**: 14529–14532.
Powell DR, Smith M, Greer J, Harris A, Zhao S, DaCosta C, Mseeh F, Shadoan MK, Sands A, Zambrowicz B, et al. (2013) LX4211 increases serum glucagon-like peptide 1 and peptide YY levels by reducing sodium/glucose cotransporter 1 (SGLT1)-mediated absorption of intestinal glucose. *J Pharmacol Exp Ther* **345**:250–259.
Pribanic S, Gisler SM, Bacic D, Madjdpour C, Hernando N, Sorribas V, Gantenbein A, Biber J, and Murer H (2003) Interactions of MAP17 with the NaPi-IIa/PDZK1 protein complex in renal proximal tubular cells. *Am J Physiol Renal Physiol* **285**:F784–F791.
Shibazaki T, Tomae M, Ishikawa-Takemura Y, Fushimi N, Itoh F, Yamada M, and Isaji M (2012) KGA-2727, a novel selective inhibitor of a high-affinity sodium glucose cotransporter (SGLT1), exhibits antidiabetic efficacy in rodent models. *J Pharmacol Exp Ther* **342**:288–296.
Vernaleken A, Veyhl M, Gorboulev V, Kottra G, Palm D, Burckhardt B-C, Burckhardt G, Pipkorn R, Beier N, van Amsterdam C, et al. (2007) Tripeptides of RS1 *(RSC1A1)* inhibit a monosaccharide-dependent exocytotic pathway of Na^+-D-glucose cotransporter SGLT1 with high affinity. *J Biol Chem* **282**:28501–28513.
Veyhl-Wichmann M, Friedrich A, Vernaleken A, Singh S, Kipp H, Gorboulev V, Keller T, Chintalapati C, Pipkorn R, Pastor-Anglada M, et al. (2016) Phosphorylation of RS1 (RSC1A1) steers inhibition of different exocytotic pathways for glucose transporter SGLT1 and nucleoside transporter CNT1, and an RS1-derived peptide inhibits glucose absorption. *Mol Pharmacol* **89**:118–132.
Vrhovac I, Balen Eror D, Klessen D, Burger C, Breljak D, Kraus O, Radović N, Jadrijević S, Aleksic I, Walles T, et al. (2015) Localizations of Na^+-D-glucose cotransporters SGLT1 and SGLT2 in human kidney and of SGLT1 in human small intestine, liver, lung, and heart. *Pflugers Arch* **467**:1881–1898.
Wright EM, Loo DDF, and Hirayama BA (2011) Biology of human sodium glucose transporters. *Physiol Rev* **91**:733–794.
Zambrowicz B, Freiman J, Brown PM, Frazier KS, Turnage A, Bronner J, Ruff D, Shadoan M, Banks P, Mseeh F, et al. (2012) LX4211, a dual SGLT1/SGLT2 inhibitor, improved glycemic control in patients with type 2 diabetes in a randomized, placebo-controlled trial. *Clin Pharmacol Ther* **92**:158–169.
Zeuthen T, Zeuthen E, and Klaerke DA (2002) Mobility of ions, sugar, and water in the cytoplasm of Xenopus oocytes expressing Na^+-coupled sugar transporters (SGLT1). *J Physiol* **542**:71–87.

Address correspondence to: Dr. Hermann Koepsell, Department of Molecular Plant Physiology and Biophysics, Julius-von-Sachs-Institute, Julius-von-Sachs-Platz 2, 97082 Würzburg, Germany. E-mail: Hermann@Koepsell.de

Supplemental Material

A Modified Tripeptide Motif of RS1 (*RSC1A1*) Downregulates Exocytotic Pathways of Human Na^+-D-glucose Cotransporters SGLT1, SGLT2 and Glucose Sensor SGLT3 in the Presence of Glucose.

Nadine Schäfer, Prashanth Reddy Rikkala, Maike Veyhl-Wichmann, Thorsten Keller, Christian Ferdinand Jurowich, Dietmar Geiger, and Hermann Koepsell

Molecular Pharmacology

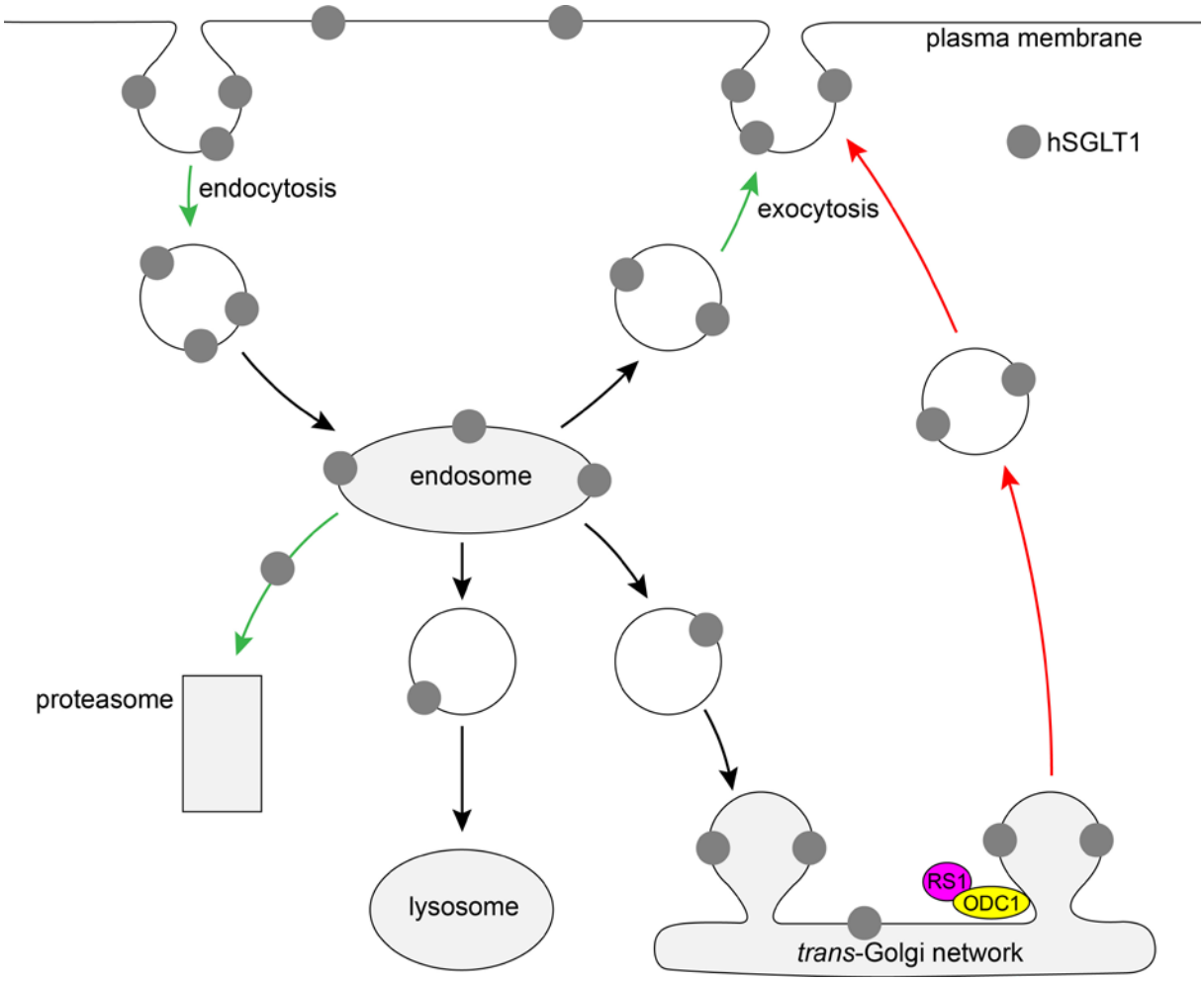

Supplemental Fig. 1. Regulation of hSGLT1 abundance in the plasma membrane. Mechanisms are depicted that can be involved in the regulation of transporter abundance in the plasma membrane. It has been demonstrated that the concentration of SGLT1 in the plasma membrane is influenced by endocytosis, exocytosis, proteasomal degradation (green arrows) and by effects on the release of vesicles from the *trans*-Golgi network (red arrows). The release of SGLT1 containing vesicles from the Golgi is regulated by RS1 via inhibition of ODC1 activity (for review see Koepsell, H. 2017 *Pharmacol Ther* **170**:148-165).

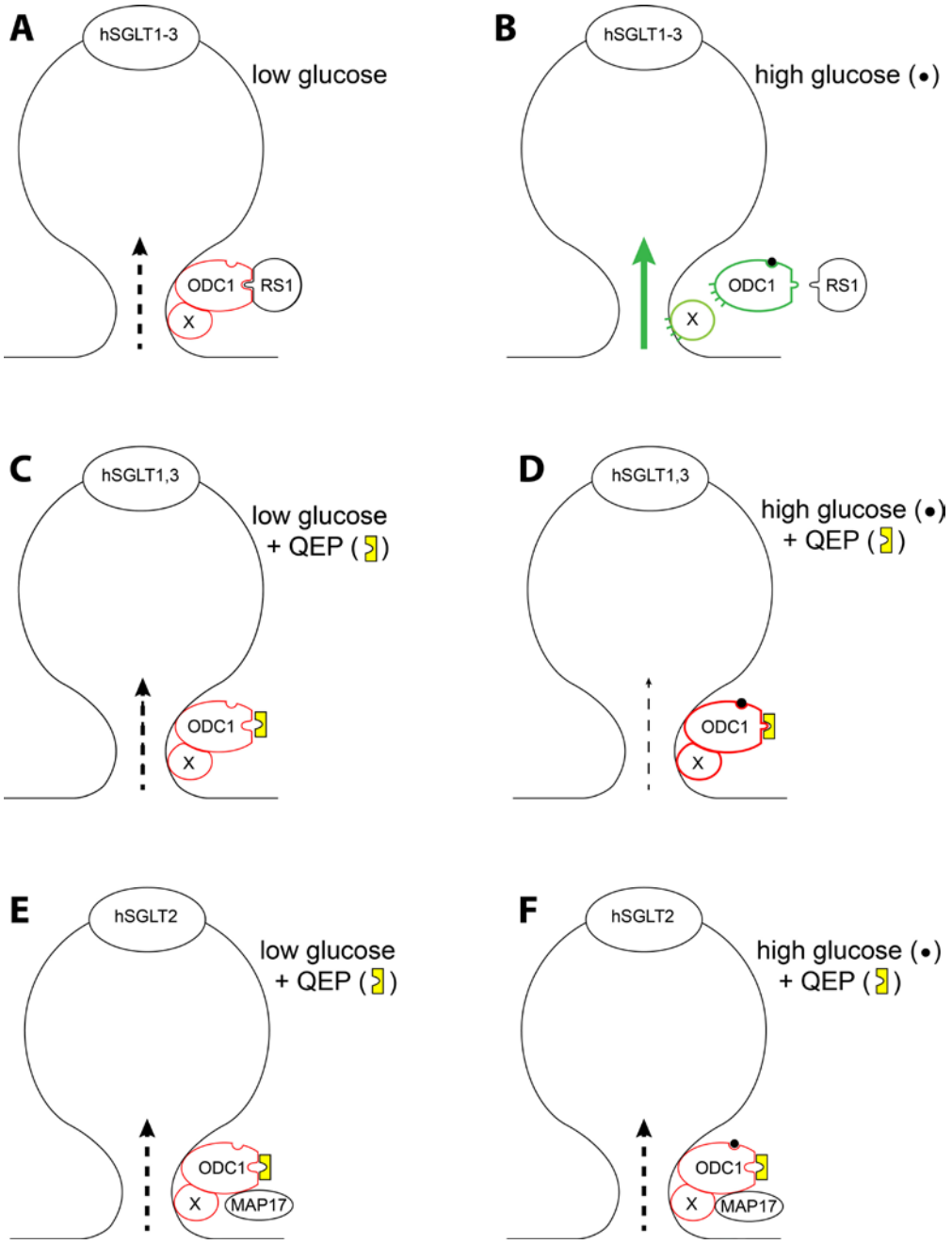

Supplemental Fig. 2. Tentative models describing how the release of vesicles containing hSGLT1, hSGLT2 and hSGLT3 from the *trans*-Golgi network (TGN) may be regulated by RS1 or QEP at low and high intracellular glucose concentrations. Deceleration of vesicle release from the TGN is induced when RS1 or QEP bind to ODC1 and inhibit the enzymatic activity of ODC1. ODC1 activity promotes vesicle release via an unknown mechanism which includes one (or several) additional protein(s) at the TGN (indicated by x). A) At low intracellular glucose concentrations when the glucose binding site of ODC1 is not occupied, RS1 binds to ODC1, inhibits the enzymatic activity of ODC1 and thereby decelerates the

release of vesicles containing hSGLT1, hSGLT2 or hSGLT3. B) At high intracellular glucose, the glucose binding site of ODC1 is occupied and RS1 does not bind to ODC1. Under this condition ODC1 is enzymatically active and promotes the release of hSGLT1 containing vesicles from the TGN. C, E) At low intracellular glucose, QEP binds to RS1 and blocks ODC1 activity. Under this condition the release of vesicles containing hSGLT1, hSGLT3 (C) or hSGLT2 where MAP17 is supposed to be associated with ODC1 (E), is slowed down. D) In cells expressing hSGLT1 or hSGLT3 where MAP17 is not involved in the regulation at the TGN, QEP binds with higher affinity to the configuration of the RS1 binding site of the ODC1-glucose complex (high intracellular glucose) compared to ODC1 with an empty glucose binding site (low intracellular glucose). At an appropriate intracellular QEP concentration a more pronounced deceleration of release of vesicles containing hSGLT1 or hSGLT3 is observed at high versus low intracellular glucose concentrations. F) The efficacy for downregulation of hSGLT2 by QEP observed after coexpression of hSGLT2 and MAP17 in oocytes may be similar in the absence and presence of glucose because MAP17 which is supposed to be associated with ODC1, may prevent the allosteric effect of glucose binding to ODC1 on the RS1 binding site.

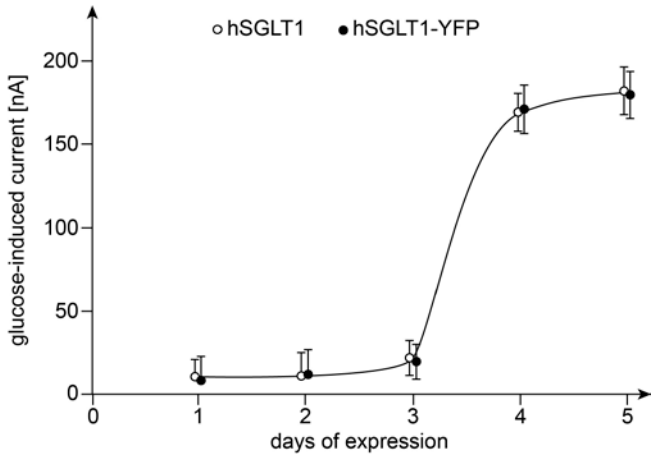

Supplemental Fig. 3. Influence of the incubation time after injection of hSGLT1 cRNA or hSGLT1-YFP cRNA into oocytes on the expression of hSGLT1. Oocytes were injected with 25 ng of hSGLT1 cRNA or 25 ng of hSGLT1-YFP cRNA and incubated for different time periods for expression. For analysis of hSGLT1 mediated currents, the oocytes were clamped to -50 mV and steady-state short-circuit inward currents observed after superfusion with 100 mM D-glucose were measured. Mean values ± S.D. of 9 oocytes are indicated. The oocytes were obtained from three different frogs.